13. DOUBLE AND MULTIPLE STAR TREATMENT

The Hipparcos Catalogue comprises a significant amount of data related specifically to double and multiple star systems, the analysis of which was a major challenge to the data reduction consortia. The processing of these systems differed in many ways from the methods set up for the single stars and in no other place in the data analysis did FAST and NDAC specialise more in their approach to the problem. As a consequence this chapter is arranged in dedicated sections for each consortium. The text aims at providing an overview of the algorithms developed and implemented in the context of double and multiple star analysis, demonstrating the capabilities and the limitations of these procedures, and summarising the main statistics of the solutions.

13.1. Introduction

In the preceding chapters, the observation schemes and data reductions for single Hipparcos stars have been presented. As is well known, however, a majority of all stars are in reality double or multiple. Fortunately (because they constituted a major complication of the data reductions), only a reasonably small subset with rather long periods and not too unequal masses appeared non-single when observed by Hipparcos. Roughly, doubles with a magnitude difference smaller than 4 mag and a separation above 0.1 arcsec were resolved by Hipparcos, that is, separate astrometric parameters could be obtained for each component. Some few, but interesting, short-period ($P \lesssim 5$ yr) systems were detected at even smaller separation from their moving photocentres. For all these 'effectively non-single' objects, special reduction procedures were used, in parallel with or complementary to the standard reductions.

Although specialised and complex data reductions were needed, the discovery and measurement of double and multiple objects was soon recognised as a major scientific by-product of the Hipparcos project. Apart from the obvious fact that accurate parallaxes for orbital systems provide one of the few direct means of determining stellar masses, there are also very important gains from obtaining a more uniform and complete statistical sampling of the visual binary population close to the Sun. The importance of double-star observations with Hipparcos was realised at an early stage in the planning of the mission (Lindegren 1979), and certain instrument parameters, in particular the period of the main grid, were therefore optimised with the efficient detection of double and multiple star systems in mind.

Some 9000 of the 12 000 doubles and multiples in the Hipparcos Catalogue (i.e. the output catalogue) were listed already in the Hipparcos Input Catalogue. Most of them had separations below 10 arcsec, and could be observed with a single pointing of the instantaneous field of view. Some systems with separations above 10 arcsec had two or more individual entries in the Hipparcos Input Catalogue, and the components were then pointed at individually but reduced together after the end of the mission. Apart from 3000 reasonably certain new doubles discovered by Hipparcos, there are also several thousand suspected cases, for which trustworthy elements could not be determined.

13.2. Double Star Detection

As stated above, many of the observable doubles and multiples were known and flagged in the Hipparcos Input Catalogue. For the unknown ones, there were two main discovery modes: firstly, at the individual frame level, i.e. directly from the properties of the signal recorded on the grid; and secondly, in the combined astrometric parameter determination.

In this latter case the image on the focal plane could not be distinguished from that of a point source and the signal was analyzed in the same way as that of a single star, with the basic assumption that the absolute motion was rectilinear. This assumption failed when the object was a binary star with a period comparable to or less than a few times the mission length, in which case the 'photocentre' had a sinusoidal motion on the sky superimposed on the linear motion of the centre of mass. The detection in this instance was of the same nature as that of astrometric binaries on photographic plates. Detection at the individual frame level, which is described in this section, was by far the most important.

Main Criteria

During the standard Hipparcos reductions, a five-parameter Fourier model was fitted to the photon counts from the image dissector tube. This model is valid for single stars as well as for double and multiple objects. For single stars, certain relations exist between the five parameters, which could be calibrated from the vast majority of effectively single objects. For manifestly non-single objects these relations do not generally hold, and this property was used to define statistical criteria for the detection of such objects.

Two equivalent mathematical forms of the five-parameter model were of constant use during the reductions and are given here for the sake of completeness. The first form describes the photon count rate A_k in terms of the parameters β_1 to β_5 (see Table 5.1):

$$A_k = \beta_1 + \beta_2[\cos(p_k + \beta_3) + \beta_4 \cos 2(p_k + \beta_3) + \beta_5 \sin 2(p_k + \beta_3)] \qquad [13.1]$$

where p_k is a known reference phase for each sample k. This is actually the form chosen by NDAC for the representation of the signal. The second form, which is more directly related to the physical model of the signal, reads:

$$A_k = I + B + I\,M \cos(p_k + \phi) + I\,N \cos(2p_k + \psi) \qquad [13.2]$$

in which $I + B$, IM, IN, ϕ and ψ may be regarded as the parameters. The relationship between the two representations is readily obtained as:

$$\begin{aligned} \beta_1 &= I + B \\ \beta_2 &= IM \\ \beta_3 &= \phi \\ \beta_4 &= \frac{N}{M}\cos(2\phi - \psi) \\ \beta_5 &= \frac{N}{M}\sin(2\phi - \psi) \end{aligned} \qquad [13.3]$$

These parameters were obtained at a rate of one set of five parameters per observational frame of 32/15 s, for each transit of the object across one of the two fields of view. In the second form, I is the total intensity of the source and B the unmodulated stellar background and dark current. M and N are the modulation coefficients of the first and second harmonic respectively, and ϕ and ψ the corresponding phases. Typically, for a single star, one has $M \simeq 0.72$ and $N \simeq 0.25$ and the two phases are related by $\psi \simeq 2\phi$. The equality would be strict for an instrument without optical distortion and fully achromatic. Any departure from this latter rule due to instrument imperfections was calibrated twice a day as a function of colour and position in the fields, and the phases were corrected accordingly. Thus, for the subsequent analysis it can be assumed that $\psi = 2\phi$ holds for a single star, or for the individual components of a double or multiple star. Similarly, the background count rate B was obtained from the photometric calibrations, so that the stellar intensity I could be regarded as known from the observations.

In this chapter quantities related to the different components of a double or multiple star will be distinguished by indices $i = 1, 2, \ldots, n$, where n is the number of components. In order to avoid as much as possible the need for double indices, notations in this chapter differ slightly from those used in other chapters, notably Chapter 5. Thus, the modulation coefficients of the first and second harmonics are denoted M, N (corresponding to M_1, M_2 in Chapter 5), and their phases are also denoted by distinct letters ϕ and ψ (corresponding to g_1 and $g_1 + g_2$ in Chapter 5). Similarly, I and B are used for the stellar and background count rates (instead of I_s and I_b), and A_k for the total modulated signal (instead of I_k).

The modulated count rate A_k, and consequently the parameters β_1, β_2, I and B, are normally measured in counts per sample interval. They were obtained, as described in Chapter 5, by fitting the signal models to the observed photon counts N_k, using a Poissonian model for the latter. The expected number of counts in each sample is $\mathrm{E}[N_k] = A_k$. In some places I or B may be expressed in Hz, or counts per second. The two units differ by a factor equal to the sample interval $T_1 = 1/1200$ s. For instance, the NDAC rectified parameters (Section 13.7) are put on a scale where magnitude $Hp = 0$ corresponds to exactly $I = 6200$ counts per sample, or $I = 7.44$ MHz.

As a result of the linearity of the Hipparcos detector, when two or more star images were simultaneously on the sensitive part of the detector their contributions added linearly and the resulting signal had the same form as Equations 13.1 or 2. In the case of a double star the signals of the individual components are written:

$$A_{k,1} = I_1 + I_1 M_1 \cos(p_k + \phi_1) + I_1 N_1 \cos(2p_k + 2\phi_1) \qquad [13.4]$$

$$A_{k,2} = I_2 + I_2 M_2 \cos(p_k + \phi_2) + I_2 N_2 \cos(2p_k + 2\phi_2) \qquad [13.5]$$

and the total, observed signal becomes:

$$A_k = A_{k,1} + A_{k,2} + B \qquad [13.6]$$

Expanding and comparing with Equation 13.2 leads to the following relations between the observed parameters and the parameters of the stellar components:

$$I = I_1 + I_2 \quad [13.7]$$

$$IM\cos\phi = I_1 M_1 \cos\phi_1 + I_2 M_2 \cos\phi_2 \quad [13.8]$$

$$IM\sin\phi = I_1 M_1 \sin\phi_1 + I_2 M_2 \sin\phi_2 \quad [13.9]$$

$$IN\cos\psi = I_1 N_1 \cos 2\phi_1 + I_2 N_2 \cos 2\phi_2 \quad [13.10]$$

$$IN\sin\psi = I_1 N_1 \sin 2\phi_1 + I_2 N_2 \sin 2\phi_2 \quad [13.11]$$

Naturally the modulation coefficients M and N are no longer equal to their single-star values, and $2\phi - \psi \simeq 0$ no longer holds true for a multiple source.

The recognition that the observed signal departs significantly from the expected signal of a single star is the basis for the double star detection at the frame level, and various algorithms and statistical tests based on this circumstance were implemented by the reduction teams. Because there are five signal parameters, while a single star is fully characterised by two parameters (corresponding to intensity and one-dimensional position), it is possible to build exactly three basically independent detection criteria from a comparison of the observed parameters with the expected single-star values. All three criteria, in slightly different forms, were used by both reduction consortia, and their main properties are explained in the following paragraphs and in Figures 13.1–13.3.

The first two criteria can be described in terms of the signal parameters β_4 and β_5 in Equation 13.1. From Equation 13.3 it is seen that for a single star, after elimination of the calibrated instrumental variations, one should have $\beta_4 = \widetilde{N}/\widetilde{M}$ and $\beta_5 = 0$, where $\widetilde{M}$ ($\simeq 0.72$) and $\widetilde{N}$ ($\simeq 0.25$) are the calibrated modulation coefficients for single stars. Both $\widetilde{M}$ and $\widetilde{N}$ depend significantly on the colour of the star, but by a happy circumstance their ratio, $\widetilde{R} = \widetilde{N}/\widetilde{M}$, is rather insensitive to the colour. Thus the observed parameters β_4 and β_5 can be used, separately or jointly, to detect duplicity. For instance, in NDAC their deviations from the single-star values were combined with their covariances to form a goodness-of-fit statistic, which for true singles should have a χ^2 distribution with two degrees of freedom.

The sensitivity of β_4 and β_5 to different situations can be evaluated analytically. Assuming that the same modulation ratio applies to each component separately, irrespective of their colours (i.e., $N_1/M_1 = N_2/M_2 = \widetilde{R}$), it is found that the normalised parameters $\beta_4/\widetilde{R}$ and $\beta_5/\widetilde{R}$ for the total signal depend only on the intensity ratio between the components, $r = I_2/I_1 = 10^{-0.4\Delta m}$ (where $\Delta m = Hp_2 - Hp_1$ is the magnitude difference), and the phase difference between the components, $\Delta\phi = \phi_2 - \phi_1$. From Equations 13.3 and 13.7–13.11 the following expressions are derived:

$$\frac{\beta_4}{\widetilde{R}} = \frac{1 + (r + r^2)(2\cos\Delta\phi + \cos 2\Delta\phi) + r^3}{(1 + 2r\cos\Delta\phi + r^2)^{3/2}} \equiv F_c(r, \Delta\phi) \quad [13.12]$$

$$\frac{\beta_5}{\widetilde{R}} = \frac{(r - r^2)(2\sin\Delta\phi - \sin 2\Delta\phi)}{(1 + 2r\cos\Delta\phi + r^2)^{3/2}} \equiv F_s(r, \Delta\phi) \quad [13.13]$$

The single star limit, obtained for small r (large Δm) or small $\Delta\phi$, is $F_c = 1$ and $F_s = 0$.

Figure 13.1 shows the functions F_c and F_s as functions of the projected separation (or phase difference $\Delta\phi$) and magnitude difference Δm. It can be noted that the determination of the two parameters β_4 and β_5 to some extent complement each other, since F_s is most sensitive to projected separations in intervals where F_c is relatively insensitive. However, neither parameter is sensitive to projected separations close to zero (modulo

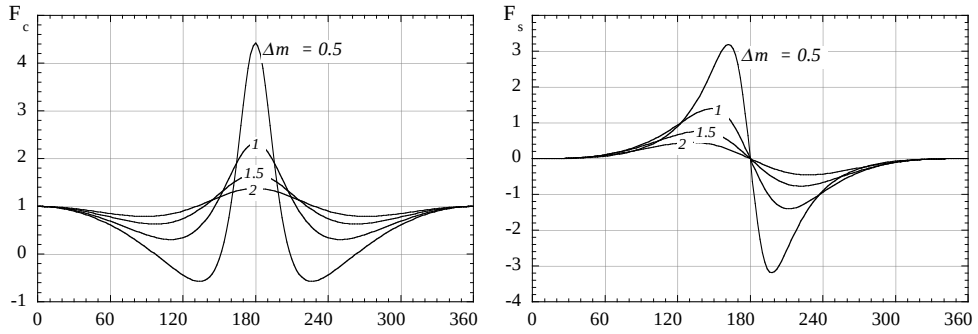

Figure 13.1. *Variation of the functions F_c and F_s with the projected separation and magnitude difference of a double star. The projected separation is measured here by the phase difference $\Delta\phi = \phi_2 - \phi_1$ between the signals of the individual stellar components; $\Delta\phi$ runs from 0 to 360° over a grid period (s = 1.2074 arcsec), see Equation 13.15. The single star limit is $F_c = 1$ and $F_s = 0$.*

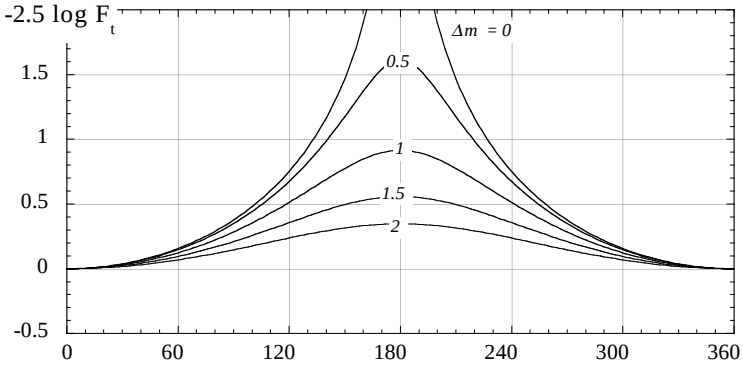

Figure 13.2. *Variation of the function -2.5 log F_t (equal to the expected value of $Hp_{ac} - Hp_{dc}$) with the projected separation and magnitude difference of a double star. The projected separation is measured by the phase difference $\Delta\phi = \phi_2 - \phi_1$ between the signals of the individual stellar components (see Figure 13.1).*

the grid period): in that case the signal cannot be distinguished from that of a single star. The typical measurement noise on $\beta_4/\widetilde{R}$ and $\beta_5/\widetilde{R}$ is of the order of 0.1 to 0.2 for a single transit, which indicates a detection limit of about 0.2 arcsec in projected separation and 2.5 mag in magnitude difference. Thanks to the accumulation of many transits in various geometric orientations over the mission, the actual limits were closer to 0.1 arcsec and 3.5 mag.

A third, independent criterion was constructed from a comparison of β_1 and β_2. Apart from the background term (which may be subtracted), β_1 represents the total intensity of the object, while β_2 represents the amplitude of the modulated intensity. For single stars the two quantities are proportional, $\beta_2 = \widetilde{M}\beta_1$, and the factor $\widetilde{M}$ could thus be calibrated as functions of time, position in the field of view, and colour index. The normalised ratio, $\beta_2/(\widetilde{M}\beta_1)$ is then close to unity for a single star. For a composite object or an extended source like a minor planet with a sizeable diameter, the degree of modulation invariably decreases, leading to a normalised ratio < 1 (Chapter 15). For historical reasons this was usually expressed in magnitude units as $-2.5\log[\beta_2/(\widetilde{M}\beta_1)]$, which

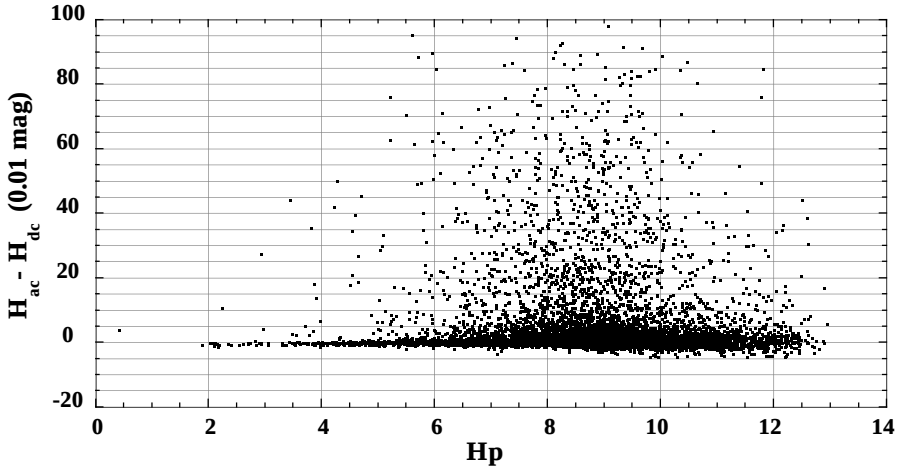

Figure 13.3. *Observed difference $Hp_{\rm ac} - Hp_{\rm dc}$ between the magnitude scales based on the unmodulated signal β_1 ($Hp_{\rm dc}$) and the modulated signal β_2 ($Hp_{\rm ac}$), plotted for the first 20 000 stars as function of the magnitude $Hp_{\rm dc}$. The detected double and multiple stars are those significantly above the line $Hp_{\rm ac} - Hp_{\rm dc} = 0$.*

corresponds to the magnitude difference $Hp_{\rm ac} - Hp_{\rm dc}$ of the Hipparcos Photometric Catalogue (see also Chapter 14).

For a double star with intensity ratio r and phase difference $\Delta\phi$ the following expression is obtained:

$$\frac{\beta_2}{\widetilde{M}\beta_1} = \frac{(1 + 2r\cos\Delta\phi + r^2)^{1/2}}{1 + r} \equiv F_t(r, \Delta\phi) \qquad [13.14]$$

The quantity $-2.5\log F_t$ ($= \mathrm{E}[Hp_{\rm ac} - Hp_{\rm dc}]$) is shown in Figure 13.2. It can be seen that it is always positive, implying that the testing for duplicity is unilateral. The observed distribution of $Hp_{\rm ac} - Hp_{\rm dc}$ for the first 20 000 Hipparcos entries is shown in Figure 13.3 as a function of the star magnitude. The central and most populated distribution is associated with single stars while the scattered population with $Hp_{\rm ac} - Hp_{\rm dc}$ significantly positive corresponds to the stars detected as non-single by Hipparcos. The width of the negative distribution provided a reliable estimate of the acceptance region for the null hypothesis.

The Hipparcos Double Stars

There were several detection limits which restricted the capability of the instrument and data reductions to recognise that a light source was not point-like. When a star was detected as non-single it was categorised as double or multiple, otherwise it was considered as single within the Hipparcos data analysis, although it may in reality be double.

Regarding the small separations, diffraction sets the limit at $\varrho > 0.10$ to 0.12 arcsec. Double stars with smaller separation went unnoticed by Hipparcos and were processed in the same way as the single stars without impairing the astrometric solution, except for short-period astrometric binaries. The separation limit depends however also on the magnitude difference of the components: detection close to the diffraction limit was only achieved for small magnitude differences (see Equations 13.40–13.41).

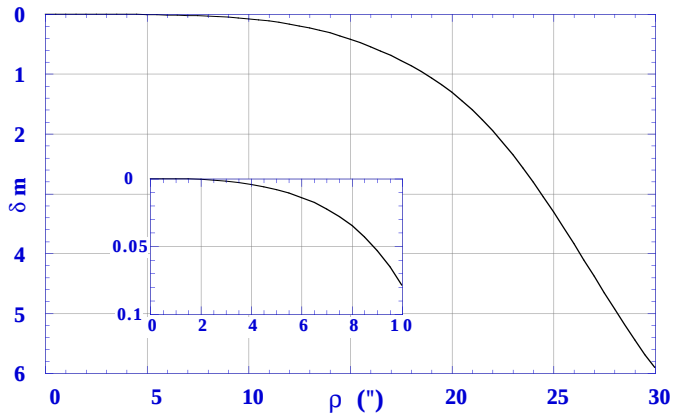

Figure 13.4. *Normalised attenuation profile of the instantaneous field of view, $\Psi(\varrho)$, as function of the distance ϱ from the centre of the instantaneous field of view. The attenuation is expressed in magnitudes. Inset: close-up of the upper left region.*

As for the large separations, only companions within some 20 to 30 arcsec from the primary could be detected, depending on the magnitude difference. This instrumental limitation followed from the use of an image dissector tube with a sensitive 'instantaneous field of view' having a nominal diameter of 38 arcsec. Actually, the sensitivity decreases gradually from the centre of the instantaneous field of view, causing an attenuation of stellar images not properly centred. For instance, a star 20 arcsec off the centre of the instantaneous field of view would appear about 1.5 mag too faint. A plot of the attenuation profile $\Psi(\varrho)$, as adopted in the data reductions and expressed in magnitudes, is shown in Figure 13.4. If the detector was pointed at the primary of a double star system, the secondary (at separation ϱ) looked fainter by $\Psi(\varrho)$ magnitudes, and the probability of its detection became correspondingly smaller. For well-resolved binaries the detection limit in magnitude difference is about $\Delta m \simeq 4$ mag, including the attenuation effect. Pairs with $\varrho \gtrsim 25$ arcsec thus generated signals hardly discernible from those of single stars, and were consequently treated as single.

Both reduction teams followed the principles laid out above, however with significant differences in the implementation depending on the local organisation of the data flow. The details of the calibrations were defined independently in each consortium and eventually resulted in different detection levels according to separation and magnitude difference. It must be stressed that the number of accepted or suspected double stars depends strongly on the thresholds set in the various tests. Depending on the adopted criteria, anywhere between 10 000 and 20 000 objects could have been accepted as non-single. At the end a fairly conservative policy was adopted: only double stars detected by both consortia and with astrometric and photometric solutions in good agreement were categorised as reliable solutions; other cases were flagged as less reliable solutions, or simply as 'suspected non-singles' without providing a double-star solution. A summary of the number of solved or detected non-single stars is given in Table 13.1. Of the 18 800 entries solved as non-single by at least one of the consortia, only about 13 200 were finally included in Part C of the Double and Multiple Systems Annex. All the remaining entries (some 8150) either had other kinds of double-star solutions (Part G,

Table 13.1. Number of entries solved as double stars by each consortium, and the number of unsolved but possibly double systems, divided into detected cases and those only detected by the other consortium.

		FAST			
		Solved	Detected	Undetected	Total
NDAC	Solved	12710	1030	2250	15990
	Detected	500	210	2190	2900
	Undetected	2310	160	–	2470
	Total	15520	1400	4440	21360

O or V) or were flagged as 'suspected non-singles' in the main Hipparcos Catalogue (Field H61).

13.3. The Astrometric and Photometric Solution: FAST Method

In the FAST processing of double and multiple stars, a relative astrometric and photometric solution was first built. This was then used as an input to the main algorithm of the absolute astrometry, i.e. the same algorithm as used for the single stars. The required input consisted mainly of the corrections to be applied to the great-circle abscissae as if the point observed on the grid had been the primary star or, for a close pair, the photocentre. This section therefore describes separately the processing for the relative astrometry, the relative photometry, and the absolute astrometry.

The FAST method contrasts with the NDAC method where the double and multiple stars were processed in a chain fully independent of the single star processing, by fitting the absolute astrometry and photometry directly to the parameters derived from Equation 13.2.

The Relative Astrometry of Double Stars

From the fitted five-parameter model, Equation 13.2, it was possible to solve, in each field transit, for the projected difference in phase between the secondary and primary component, $\Delta\phi = \phi_2 - \phi_1$. The geometry of the problem is sketched in Figure 13.5. In Equations 13.8–13.11 the left-hand sides were known from the observations at the frame level and were calibrated to account for the inhomogeneity of the sensitive surface. The right-hand sides comprise four unknowns: the two intensities and the two phases. The ratio I_2/I_1 is directly related to the magnitude difference, and the phase difference $\phi_2 - \phi_1$ is linked to the projected separation in the scanning direction, $\Delta G = \varrho \cos(\gamma - \theta)$, according to:

$$\Delta\phi = 2\pi \bmod(\Delta G/s,\ 1) \qquad [13.15]$$

where $s = 1.2074$ arcsec is the angular size of the grid period (or grid step).

For every transit Equations 13.8–13.11 were solved for the intensity ratio and the phase difference $\Delta\phi$ by a numerical method based on an adapted Newton-Raphson algorithm for non-linear systems. To avoid statistical bias, several transits were combined together,

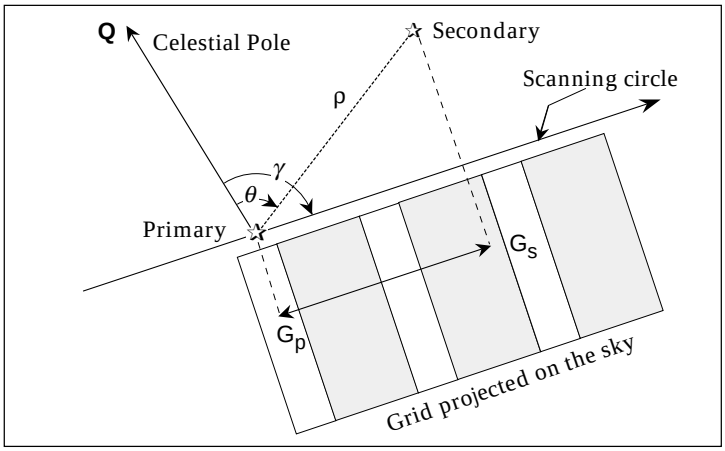

Figure 13.5. *Geometry of the observation of a binary star with separation ϱ and position angle θ as seen from the outside the celestial sphere. The angular coordinate along the scanning circle is denoted G. The signal observed depends only on the projected phase difference $\Delta\phi$ between the phase of the secondary (at G_s) and that of the primary (at G_p). The orientation of the scanning circle is indicated by γ.*

provided the geometry (angle γ in Figure 13.5) did not change too much over the timespan involved in this combination. The number of transits combined depended also on the separation of the double star. For wide pairs, the combination was always limited to the two consecutive transits, respectively in the preceding and following fields. For a separation of the order of 0.3 arcsec the precision of the phase difference in this step was in the range of 10 to 50 mas. It was also noted that for small projected separations, it happened that the sign of the phase difference remained largely undetermined, while its magnitude was correct. This is equivalent to saying that in such a configuration the position angle of the binary had a 180° ambiguity. In some sequences of observations, when the orientation of the binary on the sky remained more or less parallel to the grid slits for many transits, the projected separation could remain very small. Consequently there was a risk of having inconsistencies in the set of phase differences. A special treatment was implemented in the final step of the relative astrometry solution to identify these transits and reverse the sign of the phase differences $\Delta\phi$.

The relationship, Equation 13.15, between the projected phase difference ($\Delta\phi$) and the projected angular separation (ΔG) indicates that the detector signal only provides information on ΔG to within an integral number of grid periods and that the possible ambiguity for separations larger than the grid period had to be resolved at a later stage of the processing.

At the end of the above steps all the projected phase differences, $\Delta\phi_j$ ($j = 1, \ldots, m$), were known together with the orientations γ_j of the scans on which they were obtained. The final step consisted of finding the relative astrometry, ϱ and θ, that accounted for the observed $\Delta\phi_j$. In the jth observation the projected separation on the Hipparcos grid was:

$$\Delta G_j = \varrho \cos(\gamma_j - \theta) \qquad [13.16]$$

In terms of the rectangular coordinates $X = \varrho \sin\theta$ and $Y = \varrho \cos\theta$ of the secondary with respect to the primary, the projected separation is also written:

$$\Delta G_j = X \sin\gamma_j + Y \cos\gamma_j \qquad [13.17]$$

Subsequently it is convenient to use, instead of the angles γ_j, the components of the main spatial frequency of the grid along the X and Y axes:

$$\begin{aligned} \alpha_j &= (2\pi/s)\sin\gamma_j \\ \beta_j &= (2\pi/s)\cos\gamma_j \end{aligned} \qquad [13.18]$$

From Equations 13.15 and 13.17 the set of m observation equations can now be written:

$$\Delta\phi_j = \mathrm{mod}(\alpha_j X + \beta_j Y,\ 2\pi) \qquad [13.19]$$

in which the unknowns are the relative coordinates of the binary (X and Y), and the observational data are the phase differences $\Delta\phi_j$ derived from the signal parameters.

A special minimisation procedure was developed to find the values of X and Y which made the norm of the vector of the residuals as small as possible. For this purpose it is easier to use the following two equations, which taken together are equivalent to Equation 13.19:

$$\begin{aligned} \cos\Delta\phi_j &= \cos(\alpha_j X + \beta_j Y) \\ \sin\Delta\phi_j &= \sin(\alpha_j X + \beta_j Y) \end{aligned} \qquad [13.20]$$

This formulation avoids the use of the discontinuous modulus function, which is awkward in minimisation algorithms, and allowed the grid-step factors to be automatically managed, without trial and error. A maximum likelihood estimator, based on an assumed von Mises distribution of the angular quantities $\Delta\phi_j$, led to searching the minimum in the $(X,\ Y)$ space of the function:

$$U(X,\ Y) = -\frac{\sum_{j=1}^{m} \kappa_j \cos(\alpha_j X + \beta_j Y - \Delta\phi_j)}{\sum_{j=1}^{m} \kappa_j} \qquad [13.21]$$

which would have been exactly -1 for a perfect fit. The weight of each observation was $\kappa_j \simeq 1/\sigma_j^2$.

The problem was thus reduced to a classical one of numerical analysis, but with some very specific peculiarities:

- $U(X,\ Y)$ has many minima in the $X,\ Y$ plane, more or less evenly distributed on a lattice with period of the order of the grid step in each direction;
- because of the noise and the possible outliers among the $\Delta\phi_j$ it happened that the deepest minimum was not necessarily the point closest to the true parameters of the binary stars;
- for large separations it proved quite important to have a starting point in order to limit the exploration of the $X,\ Y$ domain to a region of a few arcsec around this point. This saved computing resources and limited the risk of finding a false minimum far away from the true solution;
- because of the sign indeterminacy of the $\Delta\phi_j$ for the small separations and the small projected phase differences, the search was always done first for a solution with a 180° ambiguity for the orientation of the binary, that is to say without distinguishing between the double stars of relative coordinates $X,\ Y$ and $-X, -Y$. This was done by minimising the function:

$$V(X,\ Y) = \frac{1}{n}\sum_{j=1}^{m}\left[\frac{\cos(\alpha_j X + \beta_j Y) - \cos\Delta\phi_j}{\sigma_j}\right]^2 \qquad [13.22]$$

  which has the desired symmetry, $V(-X, -Y) = V(X,\ Y)$. Then the phase signs were adjusted by looking at the residuals on every transit for both solutions. Usually

one was much better than the other and the phase $\Delta\phi_j$ was changed to $-\Delta\phi_j$ when necessary;

- the second-order expansion of $U(X, Y)$ in the vicinity of the minimum yielded the covariance matrix of the parameters, and the value of $U(X, Y)$ at the minimum was directly related to the unit weight variance with the quadratic mean of the residuals equal to $2(1 + U_{\min})$;
- for stars with significant orbital motion a linear model was introduced, with relative coordinates expressed as $X + \dot{X}t$ and $Y + \dot{Y}t$; the minimum was searched in the four-dimensional space $(X, Y, \dot{X}, \dot{Y})$.

More details about the actual implementation and the numerous settings of the software can be found in Mignard (1992).

As a result of the grid-step ambiguity, several solutions were often found which fitted the observations equally well, with no real possibility of discriminating between them. In such cases, all the acceptable solutions were saved in a special file and examined individually, using several indicators supplied by the minimisation routine to help choose one solution. Ground-based measurements of the separations, when available, were also used to resolve ambiguities. For this purpose a data base was set up at the Observatory of Torino to collect the most up-to-date information on double and multiple systems. In addition, all publications of recent speckle observations were cross-checked with the Hipparcos Input Catalogue to determine the relative astrometry of a number of close binaries at the mid-epoch of the space observations.

It must be stressed however, that for the unambiguous doubles, i.e. for systems with magnitude difference $\Delta m \lesssim 2.5$ mag and separation $\varrho \gtrsim 0.2$ arcsec, the Hipparcos determination of the relative astrometry is usually very reliable, even without good *a priori* starting values. For those unambiguous cases, the main advantage of having ground-based separation values, was to make the search for a solution faster, without influencing the solution itself. For separations larger than a few grid steps, a blind search, while feasible, would have been too costly and unsafe without reasonable starting values for the separation and position angle. Hopefully, the data in the Hipparcos Input Catalogue were sufficiently reliable for this category of doubles.

The Photometric Solution

The relative astrometry and photometry were considered as two different processes in the FAST data reduction. This had the advantage of making the processing easier to handle and probably more robust, but with the drawback of neglecting important correlations between astrometry and photometry. This is particularly important for the very small separations where the errors in separation and magnitude difference become strongly correlated.

The preceding steps ended up with the relative coordinates X, Y of the components of the double star. For every grid transit ($j = 1, \ldots, m$) the scanning direction (γ_j) was also known, so the projected phase differences $\Delta\phi_j$ could be computed according to Equation 13.19. On the other hand, the normalised signal parameters $\beta_4/\widetilde{R}$ and $\beta_5/\widetilde{R}$ were also known from the analysis of the detector signal. The latter are related to the phase differences and the intensity ratio through the functions F_c and F_s defined in

Equations 13.12 and 13.13. This allowed the intensity ratio r that gave the best fit to the $2m$ observation equations to be determined, by minimising the function:

$$\chi(r) = \sum_{j=1}^{m} \omega \left(\frac{(\beta_4 / \widetilde{R})_j - F_c(r, \Delta\phi_j)}{\sigma_{c,j}} \right) + \sum_{j=1}^{m} \omega \left(\frac{(\beta_5 / \widetilde{R})_j - F_s(r, \Delta\phi_j)}{\sigma_{s,j}} \right) \qquad [13.23]$$

where $\sigma_{c,j}$ and $\sigma_{s,j}$ are the standard errors of the normalised signal parameters. $\omega(x)$ is an influence function chosen to make the statistical procedure both reasonably efficient and robust, i.e. protected against outliers. The classical least–squares method corresponds to the choice $\omega(x) = x^2$, and would have led in the present case to a one-dimensional non-linear least-squares estimate of r. It is well known that the least-squares method is very sensitive to outliers, or the contamination by observations with a more extended error distribution than the Gaussian. Several influence functions were tried before selecting:

$$\omega(x) = \log(1 + x^2/a^2) \qquad [13.24]$$

associated with the Cauchy distribution. The scale factor $a = 1.64$ was adopted as a compromise between robustness (small a) and good asymptotic efficiency (large a).

Extensive simulation software was written to test the procedures on virtually any kind of double star and to investigate the bias of this estimator. Not surprisingly there was a bias both for very small separations and for large magnitude differences. A large lookup table, containing the bias correction as a function of the double star parameters and signal-to-noise ratio, was built and incorporated into the software to supplement the estimator. The minimum of $\chi(r)$ was then obtained with the 'golden section search' (Press *et al.* 1992) after the minimum was bracketed by a discrete search.

The final step in the photometric solution was to account for the attenuation profile, $\Psi(\varrho)$, of the instantaneous field of view (Figure 13.4). In the simplest case when the detector was pointed at the primary, and the secondary was consequently at a distance ϱ from the centre of the instantaneous field of view, the corrected (true) magnitude difference was obtained as:

$$\Delta m = \Delta m' - \Psi(\varrho) \qquad [13.25]$$

where $\Delta m' = -2.5 \log r$ is the apparent magnitude difference computed from the measured intensity ratio. This formula is easily generalised to the situation when the pointing was at the secondary, or at an intermediate point between the two components, as was the case for some binaries with known separations around 10 arcsec.

While more than 22 000 Hipparcos entries were recognised as probably non-single objects, there were only about 16 800 for which a solution for the relative astrometry could be derived with some reliability. The magnitude differences were then computed as described above for all these objects. The final catalogue includes a significantly smaller number of solutions since a rather conservative policy was adopted for the merging of the FAST and NDAC solutions (see Section 13.7).

Results of the FAST Solutions

Two different software packages were written and implemented, one by a group in CERGA and the second by teams in Istituto di Astrofisica, CNR, in Frascati and in Osservatorio Astronomico di Torino, which focused primarily on known double stars. The FAST solution is a merge of these two solutions, adopting either solution when only one was available and some weighted mean when the two groups produced similar

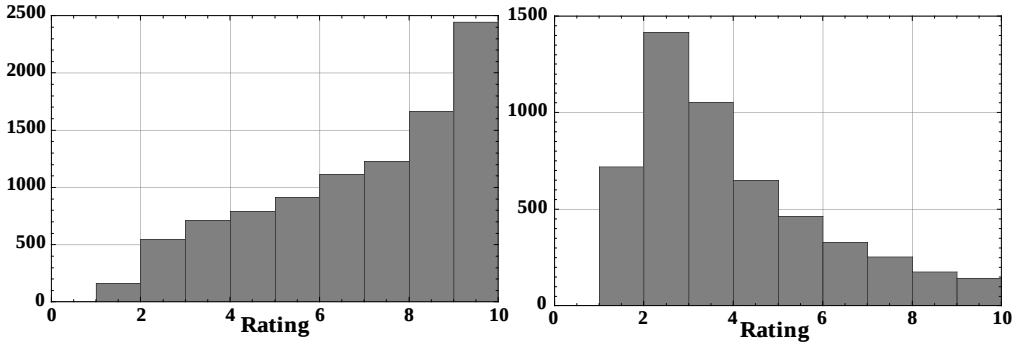

Figure 13.6. *The rating of the double star solutions in FAST, from 0 for the poor solutions to 10 for the most reliable. The distribution in the left diagram is for the systems known to be double before the Hipparcos mission while the diagram on the right refers to the double stars discovered by Hipparcos.*

solutions. When two discrepant solutions were obtained various criteria based on the ground-based separation and position angle or on the standard errors were used to select the one considered as most likely correct.

The FAST solution for the relative astrometry and photometry consisted of 16 634 entries with separation, position angle and magnitude difference together with their standard errors. Because of the two-pointing systems these solutions accounted for about 15 200 different systems: 9500 known systems and slightly more than 5500 new systems. The separation between the two groups cannot be made more precise because it would have required a careful investigation of the existing data base with the problem of cross-identification of systems and components. This has been done at the end for the final Hipparcos Catalogue. There was an additional set of 6000 entries suspected of being non-single but with no satisfactory double star solutions.

A quality factor was computed to grade each solution between 0 and 10, taking into account various factors such as the detection level, the standard errors, the number of alternate solutions, whether the convergence toward the solution was direct or tortuous, the number of phase ambiguities, etc. Solutions with a mark close to the maximum are highly reliable while a mark below or equal to 3 indicated that the quality of the solution may be questioned. The distribution of this rating is shown in Figure 13.6 for the known double stars on the left and those newly discovered by Hipparcos on the right. The two distributions differ markedly, reflecting the higher than average difficulty encountered in solving the new double stars, which were of smaller separation in general. A significant fraction of the new double stars falls in the category of low rating and this constitutes the typical set with separations in disagreement with the NDAC solution. They were eventually rejected during the merging phase (Section 13.7).

The main results obtained by FAST are shown in Figure 13.7 for the systems whose duplicity was known from ground-based observations before the Hipparcos mission and in Figure 13.8 for the new doubles stars detected and solved by FAST. One must stress that these plots refer to the FAST processing, before the final selection of double and multiple solutions based on the comparison between the FAST and NDAC solution (Section 13.7). The distribution of the separations extends up to more than 25 arcsec for the population of known double stars with a large fraction of systems with $\varrho \simeq 1$ arcsec. The separations for the new double stars is strikingly different with a maximum of

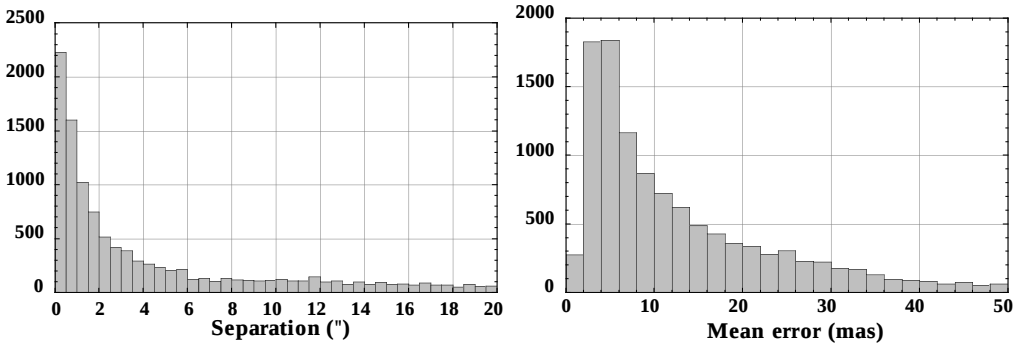

Figure 13.7. *Distribution of the separations (left) in the FAST solution for the systems known to be double before the Hipparcos mission. The distribution of the mean error is shown on the right for the same systems.*

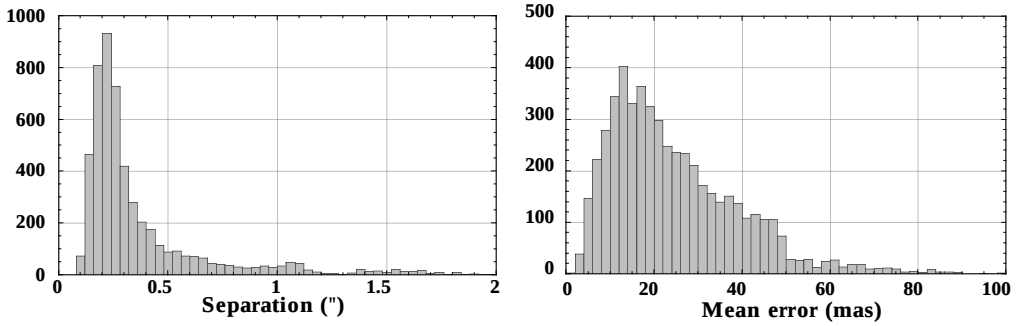

Figure 13.8. *Distribution of the separations (left) in the FAST solution for the systems discovered to be double from the Hipparcos observations. The distribution of the mean error is shown on the right for the same systems.*

the distribution at about 0.3 arcsec and very few systems above 2 arcsec. For these difficult cases, it was usual to end up with at least two solutions, one with a small separation, $\varrho \leq 0.3$ arcsec, and another one or two grid steps larger. For such a system statistics of the projected phase difference were computed over the set of transits where a positive detection had occurred. If the true separation of the double star was larger than a few grid steps, the set of phase differences was expected to be more of less uniformly distributed between 0° and 360°, while for true separations less than a grid step one expected a cluster of small values. The consistency between the observed statistics and the fitted separations eventually helped choose between alternate solutions corresponding to separations differing by one or several grid steps.

In Figures 13.7–13.8, the right panels show the distribution of the mean error on the relative position of the secondary respectively for the population of known and new double stars. Not surprisingly the first population gives a median in the error of the order of 5 mas while for the new double stars, with a much lower signal-to-noise ratio, the distribution is wider with a median value of about 20 mas.

The Multiple Stars

A dedicated treatment has been applied by FAST to process systems with more than two components and to obtain their relative astrometry and photometry. The absolute

astrometry was then derived in the same way as for either double or multiple systems and is considered in this section.

The problem of multiple star treatment is more difficult than that of double stars because, with the same amount of information collected at the level of the image dissector tube data reduction, at least three additional parameters per component must be determined: separation, position angle and magnitude difference. This must be done while the same difficulties already described for double stars (in particular grid-step errors and the indeterminacies occurring when two components are close and with similar brightness) may exist for any pair within the multiple system.

There is no criterion that could be derived from the Hipparcos data that would permit the recognition of specifically multiple systems. Actually, the same criteria used to detect double stars (Section 13.2) apply just as well to systems with more than two components, so that multiple systems are to be found among the stars recognized as non-single by the double star detection software.

Because of the larger number of unknown parameters to be determined, classes of systems for which realistic solutions could be obtained are more restricted than in the case of double stars. Not only the observability conditions stated for double stars must be satisfied by any pair of components, but they must be even more stringent: each component must provide sufficient information to be clearly recognized and separated from any other. And the larger the number of components is, the more restricted become these conditions and, assuming a given number of observations, the less chances exist to obtain a solution.

For these reasons, in FAST, only triple systems were considered and experience showed that a minimum of 25 observations (well distributed over the scanning directions) were necessary to obtain a good solution.

Selection of systems: In the absence of specific criteria to recognize multiple systems, the choice of stars to be tested with the triple star reduction software was made as follows:

- first, all stars in the Hipparcos Input Catalogue which were known to be multiple with three components obeying the double-star observability conditions for the three possible pairs. In many cases, when two of them had a small separation (< 0.25 arcsec), a double star solution in which the closest pair of stars was replaced by their photocentre was found to be more reliable;
- double stars for which no relative solution could be found without rejecting a large number of observations or for which the absolute astrometric solution was obtained with a bad goodness-of-fit or which necessitated many rejections of observations.

In FAST, two completely different methods were used:

(1) the scanning angle functions method, created and implemented in CERGA, Grasse;

(2) the global fitting method, developed at the Osservatorio Astronomico di Torino, Italy.

In addition, an application to multiple star systems of the CLEAN imaging method was studied, but not applied because the relative astrometry approach adopted in FAST for double and multiple star reduction, did not permit the definition of a common reference frame for all the observations. This was actually possible for NDAC which performed

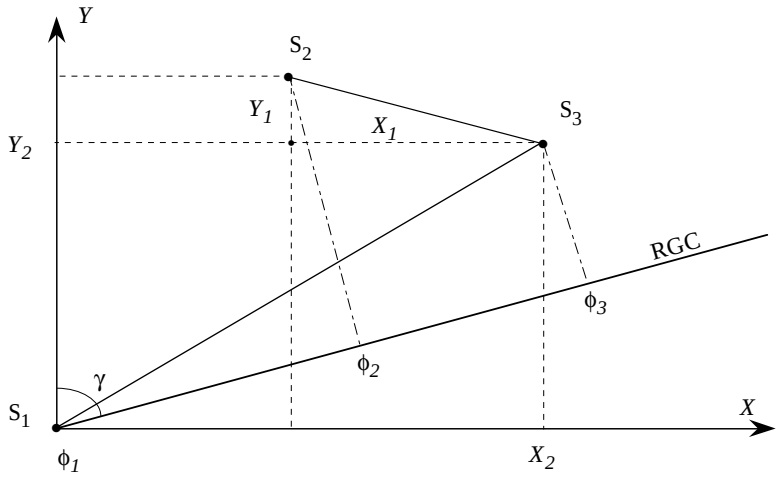

Figure 13.9. *Projections of the positions of the components of a triple system on the tangent plane and on the reference great circle whose position angle is* γ.

the reduction simultaneously with absolute astrometry so that a single reference was available for all the observations.

In the case of FAST methods, an *a priori* approximate solution was necessary to start converging toward the solution. The two methods described below differ in particular by the way that such an approximate solution is obtained.

Scanning angle functions method: The observed signal of a triple star could be represented by Equation 13.2 in which it was assumed that ψ has been corrected by the calibrated phase shift which exists for single stars as already explained in Section 13.2. The relations with the parameters of the components are extensions of Equations 13.7–13.11 with three terms rather than two. Let us consider a system of local coordinates $X\,Y$ with their origin at one of the components of the systems, S_1 (Figure 13.9). One considers the two vectors $\overrightarrow{S_1S_3}$ and $\overrightarrow{S_3S_2}$ whose coordinates are respectively (X_2, Y_2) and (X_1, Y_1).

The projections on the reference great circle, which were proportional to phases, modulo 2π, were such that for the jth observation we have:

$$(\phi_3 - \phi_1)_j = \mathrm{mod}(\alpha_j X_2 + \beta_j Y_2,\ 2\pi) \qquad [13.26]$$

$$(\phi_2 - \phi_3)_j = \mathrm{mod}(\alpha_j X_1 + \beta_j Y_1,\ 2\pi) \qquad [13.27]$$

where α_j, β_j are given by Equation 13.18. In addition, the intensities were normalised with respect to the total intensity, so that the actual intensities were determined at the very end, using the global calibrated intensity provided by the photometric treatment as:

$$J_k = \frac{\sqrt{2}\, I_k}{I_1 + I_2 + I_3}, \qquad k = 1,\ 2,\ 3 \qquad [13.28]$$

with

$$J_1 + J_2 + J_3 = \sqrt{2} \qquad [13.29]$$

With these assumptions, namely using only phase differences and normalised intensities, only three relations between the parameters were left. Any three combinations of Equations 13.8–13.11 could be used. The choice was to take:

$$\begin{aligned} F &= 1 - (M/\widetilde{M})^2 \\ G &= 1 - (N/\widetilde{N})^2 \\ H &= 2\sqrt{2}\,(M/\widetilde{M})^2(N/\widetilde{N})\sin(2\phi - \psi) \end{aligned} \qquad [13.30]$$

where F, G and H are functions of X_1, X_2, Y_1, Y_2, J_1, J_2, J_3 and γ, while $\widetilde{M}$ and $\widetilde{N}$ were as before the mean calibrated values of the modulation coefficients.

Values of the three functions were computed for each group of transits corresponding to a given orbit and reference great circle. Equations 13.30 are strongly non-linear and it was not possible to solve them by least-squares unless an approximate solution was available. In a first instance, each function F, G and H was represented by a Fourier series of γ, developed to the 10th or higher order depending on the number of observations. Then, two angles γ_1 and γ_2 were chosen and the seven Equations 13.26–13.30 were solved for the seven unknowns. The solution was obtained by successive approximations using 5th degree polynomial expansions of the equations. The coefficients of these expansions were computed analytically as functions of the seven parameters.

The choice of γ_1 and γ_2 was arbitrary, although many simulations have shown which combinations were the most efficient. Actually 12 such combinations, depending or not on the distribution of the angles γ were programmed and the solution was computed by a programme for the resolution of non–linear equations. Some combinations were rejected by the programme as impossible to solve. Others gave solutions which were used as starting point to the next step.

This next step consisted of studying how any of the solutions obtained changed when its parameters were slightly modified. This was a means of searching for a minimum of the root-mean-square residuals in the vicinity of the solution in the space of parameters. This space was not systematically scanned, which would have taken too much computer time, but tested in ten pre-determined directions. The goodness-of-fit of these new solutions and of the original one were compared, and the one that showed the best fit was retained.

At the end of this step, one had up to twelve solutions, not necessarily all different. The goodness-of-fit values were compared and the solution with the best fit was retained. Then, a new iteration was started, using the parameters of this solution as the starting point of the first step for the choice of γ_1 and γ_2. The iteration was stopped when the last retained solution did not improve the quality of the fit by at least 1 per cent.

Next the various solutions obtained for each couple (γ_1, γ_2) were compared by direct inspection. The one giving the best fit and the smaller number of rejections was kept. Observations which were systematically rejected at the 2.5σ level by the majority of solutions were suppressed and a new round of iterations was started.

If after one, or sometimes two, rounds more than 12 per cent of observations were rejected, or if there were no solutions with a goodness-of-fit smaller in absolute value than 4, it was considered that there was no solution possible for this star. Otherwise, the final best solution (sometimes two if the goodness-of-fit values were similar) were kept for the final test using absolute astrometry determination.

Global fitting method: This method is a classical iterative least-squares procedure which was applied in Torino and Frascati for the double star treatment and was extended for multiple stars. As in the case of the preceding method, one observation provides three equations of condition, chosen to be:

$$\begin{aligned} A &= I\,M \\ C &= I\,N\,\cos(2\phi - \psi) \\ D &= I\,N\,\sin(2\phi - \psi) \end{aligned} \qquad [13.31]$$

The usual assumption was that the system does not change with time, though the method could easily be extended by adding first or even second derivatives of the rectangular local coordinates X_k, Y_k ($k = 2, 3$) of the components with respect to the primary. In addition to these four unknowns, the method considered all the products $I_j M_j$ and $I_j N_j$ ($j = 1, 2, 3$) for each of the three components considered as independent.

The main idea of the method was to use a classical least-squares method to solve linearised equations of condition. The problem was that equations that link A, C and D to the actual star parameters are highly non-linear and one can start such a procedure only when one has in hand a set of parameters that represent already a reliable solution. So, the first approach of the method is a 'pre-global fitting' approach, starting from system parameters provided by ground-based observations and found in the Osservatorio Astronomico di Torino data base.

The equations were simplified taking only the six unknowns $I_j M_j$ and $I_j N_j$ and the Levenberg-Marquardt method for non-linear systems of equations. The idea was to define a χ^2 merit function and determine the parameters by its minimisation. This was successively done using the steepest descent method combined with the inverse Hessian method. This was iterated until the merit function showed instability around its minimum.

Then the global fitting which assumed that it is possible to linearise the equations with respect to the unknowns was applied. The linearisation was made by the Newton-Raphson technique, expanding Equations 13.31 by a Taylor series up to the first order:

$$A = A(\mathbf{X}_0) + \sum_{k=1}^{10} \delta X_k \left.\frac{\partial A}{\partial X_k}\right|_{\mathbf{X}=\mathbf{X}_0} \qquad [13.32]$$

where $\mathbf{X}$ is the vector of parameters and δX_k their increments from the previously estimated approximate solution $\mathbf{X}_0$. Equations 13.32 were solved by an iterative scheme with singular value decomposition algorithm, which is particularly well adapted to this type of problem for its numerical properties and stability.

The Absolute Astrometry of Double Stars

As mentioned earlier, the overall principles applied by FAST consisted in first obtaining the relative parameters of a double or multiple star (separation(s), position angle(s), and magnitude difference(s)), and then correcting each great-circle abscissa for the systematic offset between the, still unknown, signal phase of the primary and the observed phase of the whole system. After these two steps, all the relative parameters ϱ, θ and Δm were known for all the double stars. For a 'fixed solution' these parameters were sufficient to characterise the double star over the whole mission. In contrast, when a significant relative motion of the components had been detected, two additional parameters had been determined, namely the first time derivatives of the relative rectangular

coordinates, $\dot{X}$ and $\dot{Y}$ ('linear solution'). The variances of each of the above parameters were also available and were used to propagate the random errors to the corrected abscissae.

In the FAST processing of the great-circle abscissae all the stars were processed in exactly the same way, whether they were single or not. This meant that, in every observation frame, the grid coordinate (G) was computed from the phases of the five-parameter model of Equation 13.2, as if the star were single. Actually the signal phases only defined the grid coordinate modulo the grid step s, and the integral number of grid steps had to be computed from the *a priori* position given in the Hipparcos Input Catalogue, even though it could refer to a point not directly linked to the phase of the signal. Equations 13.8–13.11 provide the relationship between the observed phases (ϕ, ψ) and the phases of the primary (ϕ_1) and secondary (ϕ_2). To get the grid coordinate of the primary, the observed value had to be shifted by $\phi_1 - \phi$, and a corresponding correction was needed for the great-circle abscissa. Obviously, after this process, the corrected abscissa of the primary could still be wrong by an integral number of grid steps. This was accounted for in the astrometric processing by a mesh search dedicated to the double stars, since the number of grid steps was in general much larger for these objects than for single stars.

Equation 13.16 links the geometric parameters of the double star and the scanning direction to the projected separation on the reference great circle. Using Equation 13.15 the phase difference $\Delta\phi = \phi_2 - \phi_1$ between the secondary and primary was computed, while the intensity ratio r was obtained from the magnitude difference. The following equations were then used to translate the observed phases ϕ and ψ into the phase of the primary (ϕ_1):

$$\tan(\phi - \phi_1) = \frac{r \sin \Delta\phi}{1 + r \cos \Delta\phi} \qquad [13.33]$$

$$\tan(\psi - 2\phi_1) = \frac{r \sin 2\Delta\phi}{1 + r \cos 2\Delta\phi} \qquad [13.34]$$

From this, corrected great-circle abscissae could be computed for every great circle on which the double star had been observed. The corrected abscissae are statistically equivalent to what would have been obtained if the primary star had been observed without perturbation from the secondary.

The same kind of correction was applied to the secondary or to the photocentre of the system, with straightforward modifications. Likewise for an orbital double star, an ephemeris was computed and the instantaneous separation and position angle were used to determine the abscissa shift needed to refer the observations to the centre of mass. (The same could in principle have been done for double stars with a variable component, had an ephemeris of Δm been available.) By adding further components, it was also easy to generalise the above method to triple stars, and this was done for the absolute astrometry of these systems.

Regarding the propagation of the error estimates, this was easily done for a particular reference great circle by computing the derivatives of the phase shift with respect to the separation, position angle and magnitude difference and then adding the variances to the variance of the initial abscissa. However, there was a small difficulty here, in that the corrected abscissae could be strongly correlated (because roughly the same correction—including the same error from the relative astrometry—would apply to all great circles with roughly the same scanning angle γ). Neglecting this correlation would have resulted in an underestimation of the variances of the final astrometric parameters,

and the comparison of the astrometric variances of the primary and secondary would also have disagreed with the variances of the relative solution. To rectify this, an average correlation coefficient was computed by comparing the variance of $\phi - \phi_1$ with the variance of the great-circle abscissae; this correlation was then used to estimate the final variances of the astrometric parameters.

Extensive validations were needed to get everything working properly. Two independent solution programs were written for the astrometric parameters of the double stars. Although the routines for the abscissa shifts were identical, the determination of the position, parallax and proper motion from the corrected abscissae was based on different methods. Once the principles had been validated, one of the two programs was specialised into a systematic search for the position in a mesh extending to a distance as large as 30 arcsec from the *a priori* position. The candidate solutions were then used as starting values for the main routine, from which all the FAST solutions were eventually derived.

As for the absolute astrometry of triple stars, there was an additional check of the relative solutions carried out at this level. Several solutions for the relative astrometry were usually obtained by one or both methods described in the previous section. All these solutions were tried for the absolute astrometry and the results were compared with the results obtained from a double star solution or even sometimes from a single star model. A triple star solution was retained if it improved the goodness-of-fit and/or reduced the number of rejections. Also when two triple star solutions were available, the one which gave the best fit was finally retained. In total, out of more than 350 systems tested by any of the methods, 170 were accepted by at least one of the triple star programs, but after passing the absolute astrometry test, only 102 solutions were selected to be merged with the NDAC solutions.

13.4. The Astrometric and Photometric Solution: NDAC Method

The key idea for the NDAC double-star treatment was established by L. Lindegren in 1985. Instead of making the doubles behave like the single stars, by correcting the abscissae, the known or suspected non-singles were passed through a completely independent chain of reductions. In this way, the standard reductions were freed from possible contamination, and the double-star reductions could be made on a case-by-case basis. This required a certain time-lag, in that the main reduction had to be completed first, and the calibrations obtained were subsequently used to derive calibrated observations for the non-single objects.

These calibrated observations were collected into self-contained ‘case history files’, each one containing all the observations for a given object. All subsequent reductions for that object, whether it was modelled as a single, double or multiple star, needed only the case history file as input for the model fitting. Normally, a standard double-star model was first tried, and if that failed, more refined models could be tried. This general strategy proved to be very useful, not least in enabling new solutions to be rapidly computed for individual objects identified as problematic during the later stages of the reductions. The case history files have been archived, in a slightly transformed version, as the Transit Data File described in Volume 1 (Section 2.9), and are thus available for future re-examination of the solutions for about a quarter of all the Hipparcos Catalogue entries. Similar files have been also archived within the FAST Consortium.

The above strategy separated naturally the NDAC double-star reductions in two main tasks. First, all the case history files were generated, using the best calibration data available. This had to be done in a single batch by going through all the observations in chronological sequence. Then, the actual solution searches could be performed, for one system at a time. Since several reductions were carried out in sequence, using a successively larger amount of observational material (the 12-month, 18-month, 30-month, and 37-month solutions), there were equally many (or more) separate generations of the case history files, and corresponding intermediate double-star solutions.

Generation of Case History Files

The task of obtaining the case history files from the actual satellite data was a large and complex one, and the final double-star results depended critically on its correctness. There were many details and problems to be solved in the process, and only an overview can be presented here.

The input to the generation of case history files had two large and many smaller components. The largest data set consisted of the original five-parameter fits to the image dissector tube counts (β_1 to β_5 in Equation 13.1), together with their information matrices (i.e. the inverse covariance matrices). These parameters, available from the image dissector tube processing carried out at the Royal Greenwich Observatory in Cambridge (Chapter 5), had to be calibrated geometrically and photometrically before being assembled in the case history files. Most importantly, the signal phases (β_3) had to be put on an absolute scale, so that $\beta_3 = 0$ corresponded to a certain point on the sky, with known astrometric parameters. A fundamental input for this was the frame-by-frame spin phases, i.e. the along-scan attitude angle as a function of time, derived in the great-circle reductions performed at Copenhagen University Observatory (Chapter 9). These two inputs were each a couple of gigabytes in size. Smaller but equally important inputs were the geometric instrument parameters, determined once per orbit ($\simeq$ 10.7 hour interval) as part of the great-circle reductions, the time-dependent photometric calibration parameters from the photometric processing (Chapter 14), and the abscissa zero points from the sphere solution (Chapter 11).

Ideally, it would have been useful to have a case history file for every entry in the Hipparcos Input Catalogue. Because of the large amounts of data involved, this was not practical, and an important part of the process was to select the subset of known and suspected non-singles for which the case history files should be derived. This subset evolved over the successive generations of case history files, taking into account also the detections reported by the FAST consortium, so that in the end it could be assumed with some confidence that only stars that could be passed as single in the main reduction chain had not been included. Known doubles and multiples were extracted from the Hipparcos Input Catalogue and from later compilations, and were automatically included in the subset. From the different statistical criteria described in Section 13.2, a similar number of suspected non-single objects was also included. As an important check, case history files were also derived for several thousand *bona fide* single stars, enabling more direct comparisons with the ordinary single-star reductions.

The main steps of the generation of the case history files can then be summarised as follows:

1. a special version of the Hipparcos Input Catalogue was created with some key data for each entry. For two- and three-pointing systems, a primary was designated, becoming the identification for the whole system. The photocentre of the system was calculated from the available Hipparcos Input Catalogue data, and this (with an assumed parallax and proper motion, also taken from the Hipparcos Input Catalogue) defined the reference point on the sky to which all observations of the system were referred;
2. a dedicated process was used to select the systems that should have their case history files derived. In its final version this list included about 13 500 known double or multiple systems, 14 400 suspected doubles from the NDAC criteria, and 5000 *bona fide* single stars. 4400 more objects were added as being suspected by FAST, or in previous NDAC solutions;
3. the tapes with original signal parameters (β_j) for all stars were then read through, to extract the data related to the objects selected for the case history files;
4. most of the calibration data were then collected in a single direct-access file, with one record per orbit or great-circle reduction. This included the geometric instrument parameters, specifying the large-scale field-to-grid transformations, the abscissa zero points from the sphere solution, the photometric calibration parameters, and estimates of the background count rate (B in Equation 13.2) for every $\simeq 2$ min of time. The calibration file contained also the geocentric velocity and position of the satellite used for correcting stellar aberration and calculating the parallax factors;
5. the main calculations were made by a single program. Using the attitude spin phases and the geometric and photometric calibrations, the signal parameters β_j for each field transit of an object were transformed to the calibrated parameters b_j described below, referring to an accurately specified scanning geometry;
6. at this stage the output was still in chronological order, with the transits of a given system scattered in the file. This was then sorted according to the system identifiers, resulting in one case history file per system.

In order to refer the observed phases to the adopted reference point, the detailed geometrical model of the field-to-grid transformation was needed, as well as the attitude angles and in particular the spin phases (along-scan attitude). As already mentioned, these data came from the great-circle reductions, but with the spin phases corrected for the abscissa zero points determined in the sphere solution. The sphere solution supplied also the time-varying chromaticity and some subtle phase shifts depending on the sixth harmonic of the satellite spin angle. Care was needed to apply correctly the first- and second-order relativistic stellar aberration (using the known motion of the satellite) and the gravitational light deflection due to the Sun. The photometric sensitivity variations over the field of view and over time were large (several tens of per cent), and again care had to be exercised to derive values calibrated at the millimagnitude level (see Chapter 14). The whole chain was accepted as correct only after passing the stringent test of giving astrometric data for the *bona fide* single stars in almost perfect agreement with the (independent) standard astrometric solution.

All calibrations, especially for the image dissector tube sensitivity, depend on colour, which gives two kinds of problems. On the one hand, the mean colour assumed in the reductions often differs from the more accurate values now available. This can be

rather simply corrected, however, using some auxiliary output in the case history file. On the other hand, there is a more fundamental problem for single-pointing doubles with two components of unequal colour: the mean of the calibrations is not necessarily equal to the calibration based on a mean colour. When the individual colours and intensities are known, a re-derivation of case history files would in principle be possible, but the amount of work involved makes this very impractical. Also, for most of the close Hipparcos doubles, the individual colours are not known, and the differential colour problem had to be left unsolved.

Interpretation of Calibrated Data

For a given object, the case history file contained the calibrated signal parameters for all the field transits of the object collected over the mission. By calibrated it was meant that all known variations of the instrument response and attitude had been taken into account, so that the parameters could be interpreted directly in terms of absolute quantities such as the astrometric parameters (in the reference frame of the corresponding NDAC sphere solution) and the magnitude *Hp*.

For each transit of the object across the field of view, the case history file gave the Fourier coefficients b_j describing the calibrated image dissector tube counts according to the general model:

$$A_k = b_1 + b_2 \cos p_k + b_3 \sin p_k + b_4 \cos 2p_k + b_5 \sin 2p_k \qquad [13.35]$$

where the reference phases p_k were now defined with origin at the reference point. The changing sensitivity of the image dissector tube over the field of view and with time was taken into account, and the background count rate subtracted, so that zero magnitude ($Hp = 0$) corresponded to exactly $b_1 = 6200$ counts per sample. The case history file also contained the variance-covariance of the coefficients b_j.

The calibrated phases and amplitudes were defined such that a point source of unit intensity at the reference point (i.e. with the astrometric parameters adopted for the reference point) produced the detector signal:

$$A_k = 1 + \bar{M} \cos p_k + \bar{N} \cos 2p_k \qquad [13.36]$$

where $\bar{M} = 0.7100$ and $\bar{N} = 0.2485$ are modulation coefficients fixed by convention. This expression defined more precisely the meaning of the reference phase p_k.

A point source at some distance from the reference point produced a signal phase-shifted with respect to Equation 13.36, so that p_k had to be replaced by, say, $p_k + \phi$ in that equation. The phase shift ϕ depended on the offset (ξ, η) from the reference point, the position angle of the scan (γ in Figure 13.5), and the effective grid period (s) for the observation in question. All these dependencies were taken into account by rigorously computing the derivatives $f_x = \mathrm{d}\phi/\mathrm{d}\xi$ and $f_y = \mathrm{d}\phi/\mathrm{d}\eta$ for each transit. In doing so, the offset coordinates (ξ, η) were regarded as barycentric, which meant that the effects of parallax and stellar aberration (differential with respect to the reference point) could not be taken into account when (ξ, η) were computed for a specific source in a specific observation. To account for a difference in parallax with respect to the reference point, the derivative $f_p = \mathrm{d}\phi/\mathrm{d}\pi$ was also computed. The total phase shift for a point source at the barycentric position (ξ, η) and with parallax $\Delta\pi$ relative to the reference point was then computed as:

$$\phi = f_x \xi + f_y \eta + f_p \Delta\pi \qquad [13.37]$$

Naturally, ξ and η could be functions of time to describe the combined effects of the proper motion and orbital motion of the components, all reckoned relative to the (in general already moving) reference point. The case history files included the factors f_x, f_y and f_p for each transit of the object. It must be noted that f_x and f_y closely correspond to the spatial frequencies α_j and β_j of Equation 13.18.

General Solution Principle

The basis for the NDAC double and multiple star analysis was the theoretical model for the calibrated photon counts of an object with n stellar components, obtained by summing the phase shifted and scaled signals, Equation 13.36, from the individual components (i):

$$A_k = \sum_{i=1}^{n} I_i[1 + \bar{M}\cos(p_k + \phi_i) + \bar{N}\cos 2(p_k + \phi_i)] \qquad [13.38]$$

Here $I_i = 6200 \times 10^{-0.4Hp_i}$ are the component intensities (expressed in counts per sample) and ϕ_i the phases relative to the reference point, calculated from Equation 13.37. Expanding the trigonometric terms and comparing with Equation 13.35 gives the following basic relations:

$$\begin{aligned} b_1 &= \sum_i I_i \\ b_2 &= \bar{M}\sum_i I_i \cos\phi_i \\ b_3 &= -\bar{M}\sum_i I_i \sin\phi_i \\ b_4 &= \bar{N}\sum_i I_i \cos 2\phi_i \\ b_5 &= -\bar{N}\sum_i I_i \sin 2\phi_i \end{aligned} \qquad [13.39]$$

Writing the phases ϕ_i in terms of the component positions (ξ_i, η_i), which were functions of time suitably parametrised to account for proper motion and orbital motion, and of the parallaxes of the components relative to the reference point, $\Delta\pi_i$, Equations 13.39 provided a set of non-linear observation equations for the intensities and geometric parameters of the components, in which the coefficients b_j were the 'observations'. With five equations per transit, there were typically some 500 to 1000 observation equations for a given system.

In principle, all that was now required was to specify the object model (number of components, form of motion for each component, constant or variable intensity, etc.), to insert the relevant parameters (unknowns) in Equations 13.39, and perform a robust, non-linear least-squares estimation of all the parameters. Combined with the parameters of the reference point this gave directly the absolute astrometry and intensity of each component, including their standard errors and the full correlation matrix.

Practical Considerations

In practice several different solution programs were set up to cope with the various kinds of objects, and many detailed considerations were necessary before the final solutions could be obtained. For the vast majority of the systems, however, a standard 12-parameter model was sufficient. This consisted, in its most general form (Table 13.2), of one photometric and five astrometric parameters for each of two components. For two-pointing systems, a correction to the assumed attenuation profile of the instantaneous field of view could be introduced as the 13th parameter. This general form

Table 13.2. Astrometric and photometric parameters solved for in the NDAC double-star analysis. Three different physical models of the double star result from the use of various constraints: without any constraints the solution is of type 'I', with $u_{10} = 0$ a solution of type 'L' results, and with $u_{10} = u_{11} = u_{12} = 0$ the solution is of type 'F'. The parameter u_{13} applies only to double-pointing systems, independent of solution type.

Parameter	Description
u_1	magnitude of primary (Hp_1)
u_2	offset (ξ_1) in α of primary from reference point
u_3	offset (η_1) in δ of primary from reference point
u_4	offset ($\Delta\pi_1$) in parallax of primary from reference point
u_5	offset ($\dot{\xi}_1$) in $\mu_{\alpha*}$ of primary from reference point
u_6	offset ($\dot{\eta}_1$) in μ_δ of primary from reference point
u_7	magnitude difference ($\Delta m = Hp_2 - Hp_1$)
u_8	relative position in α of secondary ($\xi_2 - \xi_1 = X$)
u_9	relative position in δ of secondary ($\eta_2 - \eta_1 = Y$)
u_{10}	relative parallax of secondary ($\pi_2 - \pi_1$)
u_{11}	relative proper motion in α of secondary ($\dot{\xi}_2 - \dot{\xi}_1 = \dot{X}$)
u_{12}	relative proper motion in δ of secondary ($\dot{\eta}_2 - \dot{\eta}_1 = \dot{Y}$)
$[u_{13}$	correction factor for the attenuation profile ($\simeq 1$)]

was directly applicable to optical double stars (solution type 'I', see Field DC3 in the Double and Multiple Systems Annex), and, by constraining some of the parameters to zero, to physical binaries with approximately linear relative motion (solution type 'L') and physical binaries with fixed relative geometry (solution type 'F').

The main difficulty was to choose the initial values for the model parameters. The 1.2 arcsec grid period imposed a strict 0.3–0.5 arcsec limit for the *a priori* position error in order for the least–squares adjustment to converge towards the correct position. This *a priori* accuracy was seldom available for all components of a system, and usually a double iteration had to be used to find the relevant solution. In other words, starting with a trial set of parameters, the least-squares solution was iterated some 5–8 times. If there was no convergence, the process was repeated with another set of initial parameters. In some cases, there was convergence to several different solutions with the secondary displaced by one or more grid steps, and it was necessary to choose the one which best fitted the observations. A fundamental principle in all cases was to compare also with the best single-star solution, and only accept a double-star solution if its χ^2 fit to the observations was significantly better. Along such general lines, several different analysis programs were constructed and used as outlined below.

The 12-parameter model of Table 13.2 applied rigorously only to systems with photometrically constant components. For double stars showing significant photometric variability, the double-star parameters were determined only from a subset of the data with total magnitude close to the median value. Actually, a large effort was put into a special scheme solving for the individual magnitudes at each field transit in addition to the fixed (5+5) set of astrometric parameters. Although this is straightforward in principle, it was in practice very difficult to obtain stable and reliable solutions, and most of these results had to be discarded.

For systems with $n > 2$ components, a set of $6n$ unknowns was defined in close analogy with the double-star case. Again, the first six unknowns (u_1 to u_6) were 'absolute', referring to the designated primary component, the following unknowns for the other components (u_7 to u_{6n}) were defined relative to the primary, and a final unknown u_{6n+1} took care of the profile correction, when necessary. In principle, the observation equations were derived as for the double stars, but because of the larger dimension of the system of equations and the exponential growth of the mesh searches with the number of components, multiple-star solutions were only made when reasonably accurate *a priori* parameters were available. This restriction, coupled with severe time constraints during the last stages of the data reductions, led to a relatively small number of multiple-star solutions. With a larger effort in the future, especially in trying to find new third components to known doubles, the Hipparcos data may eventually yield many more multiple-star solutions.

13.5. NDAC Implementation and Results

Most of the double-star reductions in NDAC were made by a single person, working nearly full-time on this task since 1985. In retrospect, the path towards the final results was winding and tortuous, and several interesting side-tracks had to be left unexplored. In this section some definite milestones are recorded, before the main results are described.

Pre-Launch Simulations

As early as 1985, fairly realistic simulations of the whole double-star processing were started in Lund. An important result of these experiments was the realisation that double stars with 10 to 30 arcsec separation, although problematic, could be successfully treated, and thus had not to be excluded from the Hipparcos Input Catalogue. Another result was the demonstration that the parameters for previously unknown doubles could be found by a four-dimensional mesh search over the primary and secondary positions. Also, a first solution program for multiple stars was written and found to work for up to five components. Thus, already in 1986 many of the principles applied later were already decided on, and much of the later work can be described as an implementation of these principles, taking into account all the practical details and difficulties. A summary of the assumptions included in the simulations was presented at the INCA Colloquium in Sitges (Söderhjelm 1988). This included an outline of the practical steps needed to construct the 'case history files'.

Subsequent pre-launch simulations focused on the development of the two main solution programs (for known doubles, and for seeking the companions of suspected doubles). From a series of large-scale simulations the detection capabilities of Hipparcos could be specified in detail, as a function of the double-star parameters. It was found, empirically, that the 'difficulty' in resolving a double star is mainly governed by a combination of the magnitude difference (Δm) and separation (ϱ), which was expressed by the parameter D (sometimes called Δm_{eff}):

$$D = \begin{cases} \Delta m - 20\ \log_{10}(\varrho/0.138) & \varrho < 0.10 \text{ arcsec} \\ \Delta m - 5.5\ \log_{10}(\varrho/0.32) & 0.10 < \varrho < 0.32 \\ \Delta m & \text{otherwise} \end{cases} \qquad [13.40]$$

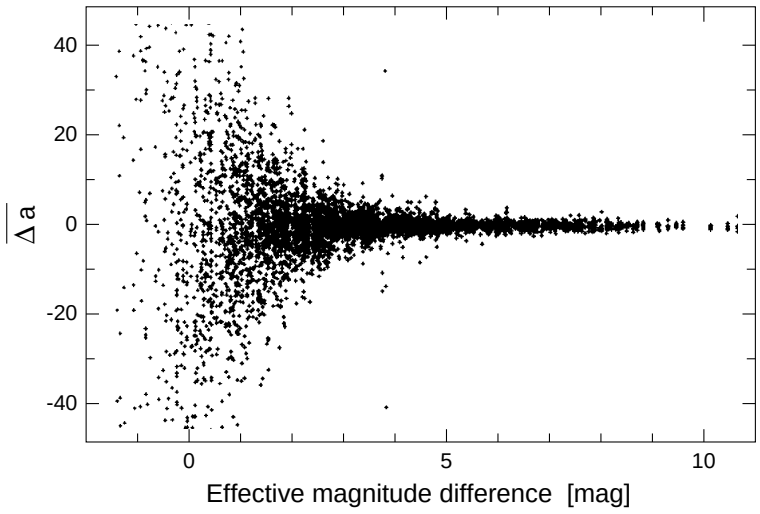

Figure 13.10. *Normalised differences, $\overline{\Delta a}$, between the double star and sphere solution results for the astrometric parameters of components of two-pointing double stars. The differences (divided by their estimated mean errors) in the five parameters are plotted against the 'observed' magnitude difference $\Delta m' = \Delta m + \Psi(\varrho)$ being the sum of the true magnitude difference on the sky (negative for a secondary component) and the attenuation when the instantaneous field of view was pointed at the other component.*

Typical diagrams showing a discovery limit for new doubles around D = 3.5 to 4 are shown in Perryman *et al.* 1989 (Volume III, Chapter 13). In 1993, the definition of D was changed to be in better agreement with the real solutions, giving instead:

$$D = \begin{cases} \Delta m - 34\ \log_{10}(\varrho/0.112) & \varrho < 0.10 \text{ arcsec} \\ \Delta m - 2.4\ \log_{10}(\varrho/0.50) & 0.10 < \varrho < 0.50 \\ \Delta m & \text{otherwise} \end{cases} \qquad [13.41]$$

First Reductions

During the spring of 1991, a small fraction of the actual observations from the first year of the mission was released to the reduction consortia in order to allow full-scale testing of the reduction procedures. In May 1991 the first solution for a 'new' double-star (HIC 927) was obtained. Within a month, the general validity of the NDAC approach had been demonstrated on the one hand by the good agreement between the single-star absolute astrometry and the independent sphere-solution results, and on the other hand by the agreement of the double-star relative astrometry with existing ground-based data. The very preliminary results for some 1000 known and 300 new doubles (Söderhjelm *et al.* 1992; Söderhjelm & Lindegren 1992) rather exceeded the expectations, and the reduction work could be continued with confidence.

In the course of the routine processing in NDAC, a new set of case history files was generated after each major sphere solution. Thus, successive versions using 12, 18 and 30 months of observations were generated during 1992–1994. In parallel, the solution programs were considerably developed and improved. As data accumulated and the detection criteria became more powerful, more objects could also be added to the list of known or suspected non-single stars, for which case history files had to be generated.

Crucially important for the validation of the absolute astrometry was a continual comparison of the double-star results with the sphere solution results for some objects which were allowed to go through both reduction chains (*bona fide* single stars, and doubles with $\varrho \lesssim 0.3$ arcsec or $\Delta m \gtrsim 3$ mag). Already in the 12-month reductions this comparison gave a good agreement in positions and parallaxes. The random differences were of the order of the standard deviations, and no systematic differences above the 1 mas level could be detected. The covariances were however found to be systematically different, reflecting the complicated correlations between the attitude-errors in neighbouring scans using a common set of 'star-mapper' stars. No rigorous model could describe this problem, but semi-empirical correction terms were introduced in the double-star solution to make the covariances reasonably similar. Another illuminating test was to compare the (disturbed) sphere-solution data for wide two-pointing doubles with the results of the double-star processing. An illustration from a May 1993 report on the 18-month results (Figure 13.10) shows the typical 'trumpet' shape of the differences, with less and less disturbance as the 'observed' magnitude difference increases. The double-star solution is able to correct for the 'mixing' of signals from both components, but only when $\Delta m'$ (Figure 13.10) reaches about 4 mag does the sphere solution give correct results. Starting with the 30-month reductions, the covariances were calibrated not only by comparison with the sphere solution, but also by making two independent double-star solutions for each object, each solution using alternate halves of the data. Magnitude-dependent correction factors were derived in such a way that the combined standard deviations of the two solutions were in agreement with the rms differences between them.

Final Reductions

A preliminary set of 37-month case history files was derived in September 1994, using 'extrapolated' results for the instrument calibrations and abscissa zero points. A large number of test solutions were made in order to settle, in particular, the covariance calibrations. The final result was a 'half-observation' scatter generally within 20 per cent of the calibrated standard errors, with no remaining dependence on magnitude, separation or magnitude difference. Another important test performed at this stage was to solve the known doubles without any *a priori* information on the relative parameters, using the solution programs developed for searching the components of a new double star. The expected solutions were recovered for a large majority of the systems, with the failure rate reaching 50 per cent only at $D \simeq 4.5$.

After completion of NDAC's final sphere solution (N37.5) in April 1995, a 'real' set of 37-month case history files were derived. After some (small) updating with photometric 'ageing corrections' in August 1995, these case history files provided the input for the final double and multiple star solutions in NDAC.

Aided by the many preliminary results, the final large-scale double-star reductions were made during the summer of 1995. In October, a systematic round of test solutions was attempted for about 1800 systems where the solutions by FAST and NDAC differed, using the FAST results as starting values. In many cases the original NDAC interpretation could be confirmed; in others, new solutions closer to those by FAST were obtained. A similar large-scale comparison with Hipparcos Input Catalogue data (which had so far not been allowed to influence the end results) generated another set of alternative solutions. Generally, however, the new solutions were retained only if they gave an improved fit to the observations, as measured by the χ^2 statistic.

For the multiple stars, solution programs had in principle been available for many years. Only after the completion of the double star processing could they be brought up-to-date, and some 180 multiple-star solutions were obtained in January 1996. In practice these solutions required rather good *a priori* relative parameters. Ideally, the large number of poor double-star solutions should also have been checked for a possible third component, but this was not accomplished in the present reductions.

In early 1996, the final merging of FAST and NDAC double-star data was made (Section 13.7). During this work, several grid-step errors were positively identified, and new solutions were calculated for individual cases. Similarly, several improved solutions were obtained by the help of dedicated ground-based observations communicated by R.S. Le Poole *et al.* (private communication). After the merging had been completed any further errors or omissions discovered, or any further improved solutions, were only listed for inclusion in the Notes to the Double and Multiple Systems Annex.

Overview of the NDAC Results

The double-star processing produced a total of 16 016 resolved double solutions. To this should be added the 180 solutions for triple and quadruple systems. For the double stars an internal quality rating was constructed, ranging from $Q = 3$ (reliable solution) to $Q = 0$ (marginal solution). This was based mainly on the parameter D in Equation 13.41 and on the improvement in fit, as measured by χ^2, from the single- to the double-star solution. The number of solutions in these quality classes were: 8415(3), 3841(2), 2485(1), 1275(0). For 14 679 additional cases, although a double-star solution was tried, a single-star solution was found to fit the data equally well. Finally, there were about 2820 systems for which no acceptable single or double star solution could be found.

For each double star, three different solutions with different constraints ('I', 'L', 'F'; see Table 13.2) were usually available, each with a complete covariance-matrix for 12, 11 or 9 astrometric and photometric parameters. Although there was in each case a preferred solution, the final selection between them was only made in connection with the merging (Section 13.7).

The NDAC approach to the double-star processing ensured that all observations collected over the mission were taken into account in a nearly optimal way, both for the detection of duplicity and for the determination of the actual parameters (absolute and relative). There was however one crucial difficulty, related to photometric variability. As described above, the NDAC solutions were made directly from the Fourier coefficients b_j in Equation 13.39, assuming constant luminosity for the components. When one or both components were variable, a model mismatch obviously resulted, and observations with important astrometric information had to be rejected. Unfortunately, this aspect of the solution process had not been tested in the early simulations, creating unexpected large problems in the reductions for variable doubles. The extensive experiments with field transit magnitudes produced in the end no useful results, but a small number of cases were noted where the secondary appeared to be the variable component.

In the standard reductions, it is clear that variability increases the probability of spurious 'new' double-star solutions, as shown by an increased number of solutions with particular values for the separation, related to the grid period of 1.2 arcsec (Figures 13.11–13.12). The detailed cause and mechanism for this problem is not well understood, but its relation to variability is shown clearly when the material is divided according

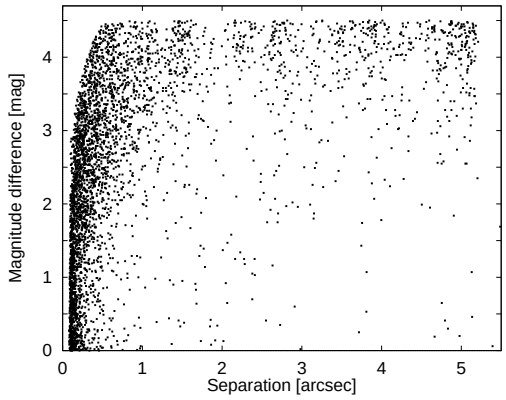

Figure 13.11. *Distribution of 'new' doubles, as obtained by NDAC, with respect to separation (ϱ) and magnitude difference (Δm). Only stars with reasonably constant total magnitude are included.*

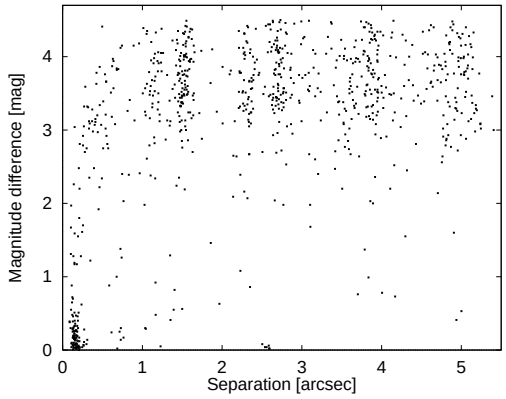

Figure 13.12. *Distribution of 'new' NDAC doubles, for the subset of stars with significantly variable total magnitude. Note the concentration of (often spurious) solutions at either small ϱ and small Δm, or to 'bands' on each side of $\varrho \simeq 1.2$ arcsec or its multiples.*

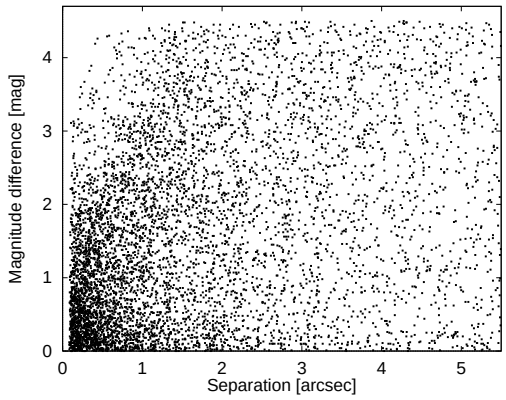

Figure 13.13. *Distribution of the NDAC solutions for 'known' doubles in the same ϱ-interval as Figures 13.11 and 13.12. No preferred separation values are apparent.*

to 'constant' or 'variable' photometry. For systems with known *a priori* parameters, there is however no similar effect, as clearly seen in Figure 13.13. (In other words, a solution in the 'band'-region may be correct, it only has an enhanced probability of being spurious). The only practical remedy for this problem has been to accept new solutions very conservatively, and for variable stars only when they are confirmed by FAST solutions. By treating the relative astrometry independently of the photometry, the FAST approach is much less liable to these problems.

13.6. NDAC/FAST Comparisons

As described above, the methods used by NDAC and FAST for the double-star processing were radically different. The two approaches had their strong and weak points, sometimes nicely complementing each other, but a major drawback has been the difficulty of making meaningful comparisons of the results. Unlike the case of single stars, there were no intermediate results that could be compared, allowing the differences in the final results to be traced back through the various stages of the processing. Throughout the comparisons, there was always a core of well-behaved objects, for which the results were in excellent agreement, but then there were also some fraction of the objects with unexpectedly large differences, and a sizable number of cases where only one of the consortia found a solution.

The first large-scale comparisons, including hundreds of solutions, were made in 1992, using solutions based on 12 months of observations. For a majority of solutions, the agreement in both the relative positions and photometry was surprisingly good, considering the radically different methods used. The differences tended to be somewhat larger than the calculated standard deviations, and some systematic effects could be seen especially in the photometry; on the whole, the agreement was however as good as could reasonably be expected. The differences were larger for the newly detected doubles, but in many cases these could be explained by grid-step errors, which, according to simulations, should be common for such a short observation interval.

A second round of comparisons was made in 1993 with the 18-month results. Again, there were thousands of stars showing good agreement in the relative data, and an effort was made to compare also the absolute astrometry (positions, proper motions and parallaxes) between the consortia. The first such attempts failed blatantly, with typically 20 to 30 mas differences in the positions, although the calculated standard errors were ten times smaller. After debugging on each side, the situation did improve early in 1994, and from then on, 'absolute' and 'relative' comparisons have shown similar differences, after normalisation by the combined standard errors, although still significantly above unity (typically 1.5 to 2). Subsequent comparisons of the 30- and 37-month results confirmed the general correctness of the solutions, but also generated lists of several thousand objects where FAST and NDAC did not agree. Big efforts were made to improve the situation, resulting in many new or alternative solutions. However, because of the very different procedures of FAST and NDAC, few of the new solutions showed radically better agreement. In the end, the remaining problem cases had to be referred to the double-star merging.

13.7. Merging of the Results for Resolved Double and Multiple Stars

Although the double-star processing in FAST and NDAC produced two sets of data, which were not always compatible, it was decided that the Hipparcos Catalogue should contain only one solution of each system. In the majority of cases, where the FAST and NDAC solutions were in reasonable agreement, this caused no problem and the published result is then essentially a mean of the two solutions ($\simeq$ 11 000 systems). Similarly, for about 6000 systems solved by one consortium but not by the other, there was no practical difficulty in accepting the one available solution, except that some criterion was needed to decide whether that solution was sufficiently trustworthy.

The greatest problem was caused by the about 1800 cases where FAST and NDAC differed very significantly in their solutions, often by a multiple of the grid step ($\simeq$ 1.2 arcsec) in the relative position of the secondary. Some 700 of these were in the end treated as single stars, or received stochastic solutions but for some 1100 entries various criteria had to be applied in order to select one of the solutions as being the most probable one (see below).

Apart from these difficulties, the merging of the results proceeded, after some initial experimentation, following a very simple recipe: a straight mean was adopted, giving equal weight to the two solutions. This averaging applied equally to the absolute and relative astrometry, and to the photometric parameters expressed in magnitudes. The main difficulty was to estimate the standard errors and, in particular, the covariance matrix of all the parameters in a merged solution.

Data Input to the Merging

The merging for the double stars was based on solutions received, in their quasi-final form, in December 1995. The FAST data consisted of:

- relative data for 16 634 entries. The following data were always included: X, Y, and Δm, with standard errors and the correlation coefficient ρ_{XY}, and a quality rating on a scale from 0 (poor) to 10 (highly reliable). For 5715 of the entries, relative motions were also provided in the form of the parameters $\dot{X}$ and $\dot{Y}$, with standard errors and the correlation coefficient $\rho_{\dot{X}\dot{Y}}$;
- the five astrometric parameters (with complete 5×5 covariance matrix) for 15 528 entries. In 5195 cases these data refer to the photocentre of the binary (where the FAST relative astrometry gave $\varrho \leq 0.35$ arcsec); in the remaining cases they refer to the primary component, or the secondary of a two-pointing system. The number of accepted and rejected observations (abscissae) and the goodness-of-fit statistic F2 were also provided with the absolute astrometry.

1155 entries thus had relative solutions but the corresponding absolute astrometry had not been accepted (e.g. because F2 > 6). The FAST relative and absolute astrometry were expressed in the ecliptical system, and a first step was to transform them to equatorial quantities (see Volume 1, Section 1.5.3), and then from the reference frame of the final FAST sphere solution (F37.3) to the provisional H30 frame by the same rigid-body rotation as was used for the merging of the single stars (see Section 17.2).

The NDAC data consisted of 15 913 entries for which the complete solution vectors (u_1 to u_{12} in Table 13.2) were given together with full 12×12 covariances. For most of the entries, all three kinds of solution (I, L and F) were given. Statistics on the number of accepted and rejected observations (field transits) and the goodness-of-fit (F2) were also given. These data referred to the equatorial system and the reference frame of the final NDAC sphere solution (N37.5); they were consequently transformed to the provisional H30 frame by the same rigid-body rotation as in the single-star merging.

An additional minor complication was that FAST and NDAC, at this stage of the reductions, used slightly different numbering systems for the catalogue entries. This affected some 80 entries. Before merging, the lists were transformed to the final numbering system of the Hipparcos Catalogue.

The Neutral Point

The content and format of the Double and Multiple Systems Annex had been worked out and agreed upon before the merging of the double star data started. Since the most complex model of the resolved systems involving orbital motion would only include the linear terms of the relative motion, it was evident that each component could be described by the same five parameters as used for single stars. The format of the Annex was therefore modelled, as far as applicable, on the format of the main Hipparcos Catalogue. The main complication to be considered was the existence of correlations between the astrometric parameters of the different components in the same system, and between these parameters and the magnitudes of the components. The correlations are often very considerable, and essential for estimating the standard error of any quantity calculated from the component data, such as the photocentre. Consequently, the Annex should list all the correlations between the astrometric and photometric parameters estimated for a given system.

The NDAC solution method provided the full covariance matrix for each system solved, and from this the required correlations were easily calculated. The FAST method, on the other hand, gave separate solutions for the relative astrometry, the relative photometry, and the absolute astrometry, and the correlations existing between the three kinds of data were not explicitly obtained. In order to merge the results properly, and to provide complete information also in the case of FAST-only solutions, it was necessary to reconstruct at least some of the correlations implicit in the FAST data. The major point to consider was to reconcile the relative and absolute astrometry.

The practical solution to this problem was based on the observation that, for sufficiently close pairs, the absolute position of the photocentre is independent of the assumed relative parameters. For well-resolved pairs, it is similarly found that the absolute position of the primary is fairly independent of the relative parameters. By generalisation it can be inferred that there is always a neutral point in a system where the absolute and relative astrometry are minimally coupled. It was assumed that this point is always located between the primary and the photocentre, the fractional distance given by a parameter q in the range from 0 (primary) to 1 (photocentre). Thus, with $\mathbf{p}$ and $\mathbf{s}$ denoting the positions of the primary and secondary, and $r = 10^{-0.4\Delta m}$ the intensity ratio, the neutral point can be written:

$$\mathbf{n} = \mathbf{p} + (\mathbf{s} - \mathbf{p}) \frac{qr}{1 + r} \qquad [13.42]$$

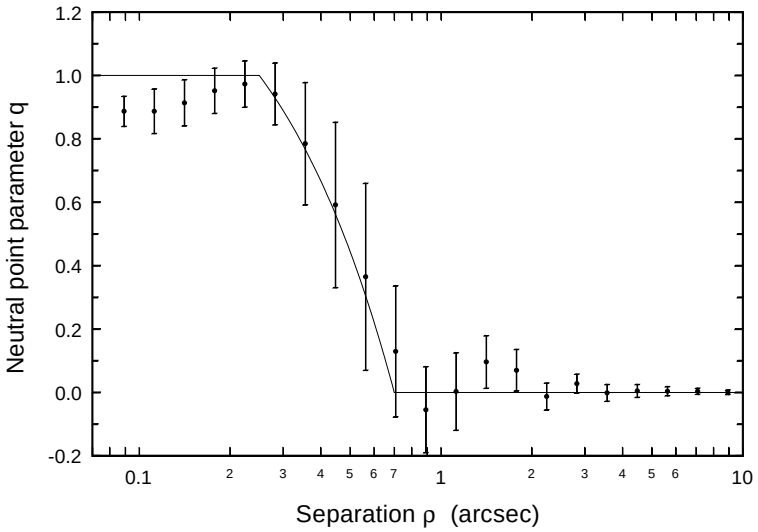

Figure 13.14. *The parameter q defines the location of the 'neutral point' as a fraction of the distance from primary (q = 0) to photocentre (q = 1). This diagram shows the determination of q versus separation (ϱ) by two completely different and independent methods: (1) the points and bars show the q-values minimising the correlation between the position of the neutral point and the relative coordinates of the components. Based on individual q-values computed from the covariance matrices of 9740 NDAC solutions, the points and bars give respectively the mean values and the $\pm 1\sigma$ ranges within each interval of separations; (2) the solid curve gives the empirical relation (Equation 13.43) minimising the positional differences between FAST and NDAC.*

The quantity q can be computed directly from the covariance matrix provided with the NDAC solutions, and is found to depend mainly on ϱ (Figure 13.14).

The neutral point was also derived empirically from a comparison of the FAST and NDAC absolute astrometry. For a set of doubles with a narrow range of separations, the q value was varied to minimise the mean positional difference between FAST and NDAC, $\langle |\mathbf{n}_N - \mathbf{n}_F| \rangle$. Repeating this process for a number of separation intervals, it was found that the best positional agreement between the consortia was obtained with a q value varying with separation roughly according to the formula:

$$q = \begin{cases} 1 & \text{for } \varrho \le 0.25 \text{ arcsec} \\ 1 - (\varrho - 0.25)/0.45 & \text{for } 0.25 < \varrho \le 0.70 \text{ arcsec} \\ 0 & \text{for } 0.70 < \varrho \end{cases} \qquad [13.43]$$

This relation is also drawn in Figure 13.14 and shows good agreement with the mean values calculated from the NDAC covariances. Based on the neutral point defined by Equation 13.43, the FAST correlations between the astrometric parameters of the components were computed such that the standard errors supplied by FAST (after modifications described below) could be recovered both for the relative positions of the components and for the absolute position of the primary or photocentre.

The concept of a neutral point was also used in order to merge the FAST and NDAC results (Figure 13.15). The relative astrometry and photometry were first merged (i.e. averaged); later, the neutral points of the two absolute solutions were also averaged, yielding the neutral point of the merged data ($\mathbf{n}_m$ in the figure). Finally, the merged separation, position angle and magnitude difference were applied to the merged neutral point, resulting in the merged positions of the components. Normally this somewhat

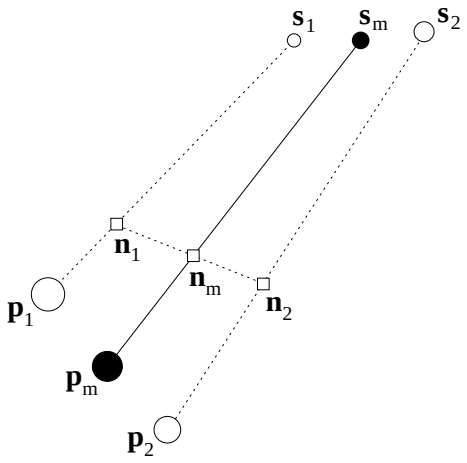

Figure 13.15. *This figure illustrates how the neutral point is used to merge the relative and absolute astrometry from the two consortia (indicated by subscripts 1 and 2). The relative parameters ϱ, θ and Δm are first averaged, yielding the merged relative locations and intensities of the components ($\mathbf{p}_m$ and $\mathbf{s}_m$). Then the neutral points are averaged to yield $\mathbf{n}_m$; finally the absolute positions of the components are obtained by applying the relative data to the merged neutral point.*

roundabout method produced virtually the same result as a direct averaging of the absolute positions of the components. However, in cases where FAST and NDAC differed significantly in Δm direct averaging could lead to unlikely results for the photocentre, which were avoided with the present method.

Discrepant Solutions

The relative astrometry and photometry were compared and merged before the (absolute) astrometric parameters were considered. The criterion for an 'acceptable' agreement included limits on the differences both in relative position and in position angle:

$$\left[(X_N - X_F)^2 + (Y_N - Y_F)^2\right]^{1/2} \leq 0.3 \text{ arcsec} \quad \text{and} \quad \left|\sin\frac{1}{2}(\theta_N - \theta_F)\right| \leq \sin 22\overset{\circ}{.}5 \quad [13.44]$$

No limit was set in $\Delta m_N - \Delta m_F$, except that Δm_N and Δm_F should both be non-negative. A limit of 0.3 arcsec was adopted for the relative astrometry, because this is approximately the maximum range over which it makes sense to average quantities which vary periodically with the grid step of 1.2 arcsec. The onset of non-linear effects at about this distance is, for instance, illustrated by the behaviour of the neutral point, which starts to depart from the photocentre, and hence from the linear regime, at a separation of 0.25 arcsec. The criterion on the difference in position angle is needed for close pairs ($\varrho \lesssim 0.3$ arcsec), where the first criterion is almost always satisfied, irrespective of the relative orientations.

Among the cases rejected by the criterion above, there was an excess of cases with $\theta_N - \theta_F \simeq \pm 180°$. If both Δm_N and Δm_F were small, this could be attributed to the noise in the magnitude differences causing a simultaneous reversal of Δm and θ in one of the solutions. In such cases the smaller of the Δm values was given a negative sign and the corresponding θ value changed by $\pm 180°$. After averaging, the resulting Δm was then still non-negative. This affected some 500 pairs.

However, in some 40 other cases the position angles differed by $\simeq 180°$ even though both Δm were strongly positive. These were almost always close pairs, and the effect was attributed to the indeterminacy of the sign of $\Delta\phi$ in the FAST reductions (see Section 13.3). Consequently, in these cases θ_F was changed by $\pm 180°$ while Δm_F was not touched.

After this 'cleaning up' of the relative astrometry and photometry, there still remained about 1400 doubles for which the FAST and NDAC solutions could not be reconciled, and for which no averaging would make sense. Several criteria were used in order to select one solution in preference to the other:

- in about 60 cases, dedicated CCD observations (Le Poole *et al.*, private communication) could definitely point out one solution as correct, and the other as incorrect;
- in about 600 cases, one solution gave a good fit in the FAST determination of astrometric parameters, while the other caused a large chi-square or many rejections. In these cases the best-fitting solution was adopted;
- a large portion of the remaining systems were individually investigated by means of the 'imaging approach' using the NDAC case history files (Perryman *et al.* 1989 Volume III, Section 14.5).

The imaging approach was found to be quite a powerful tool in the separation range of 0.2 to $\simeq 8$ arcsec, and for $\Delta m < 3$ mag. The method, in the preliminary version implemented for this specific purpose, was however very slow, and to go through hundreds of objects required a significant effort. The ambiguous cases were therefore investigated in order of decreasing importance, as measured by the FAST and NDAC quality ratings. For the highest ratings (i.e. the 'strong' doubles), a positive decision could almost always be reached. In some cases a third solution was found which was then passed as starting point for a revised NDAC solution. With decreasing quality ratings, the number of undecided cases grew rapidly, and the process was eventually terminated when the yield was too meagre. In the end some 100 cases were decided on the basis of the imaging approach, and a similar number were decided from the quality ratings alone. The remaining cases were not retained as solutions in Part C of the Double and Multiple Systems Annex: they were treated as single stars or given stochastic solutions.

All cases retained as valid double-star solutions, but with an alternative solution from the other consortium, were graded as 'uncertain' in the Hipparcos Catalogue (flag 'D' in Fields H61 and DC5). Some key parameters from the alternative solution are given in the Notes of the Double and Multiple Systems Annex (Volume 11). It should be noted that the agreement of the FAST and NDAC solutions does not preclude the possibility that both are wrong by a multiple of the grid step: the probability of this happening may be non-negligible especially for newly discovered doubles (Field H56 = 'H') with relatively poor solutions (Field H61 = 'C').

Systematic Differences

From the earlier comparison activities (Section 13.6) it was known that small systematic differences existed between the FAST and NDAC results, e.g. in the relative astrometry and photometry. Because the differences are small, especially in comparison with uncertainties in ground-based data, it has usually not been possible to ascertain that one set of data is more accurate than the other. The general principle has therefore been to accept an unweighted mean as the best compromise, also with regard to systematic

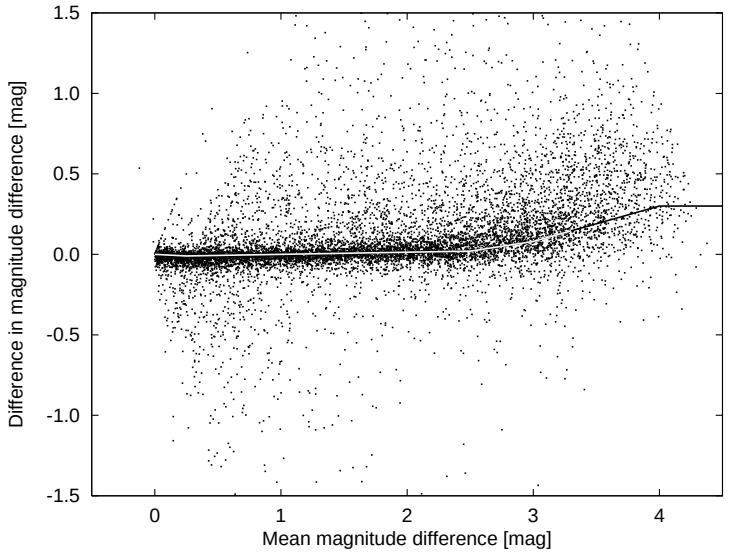

Figure 13.16. *Comparison of magnitude differences Δm as obtained by FAST and NDAC for double stars with relative astrometry in good agreement. On the vertical axis is the difference $\Delta m_{\rm N} - \Delta m_{\rm F}$, on the horizontal the mean value $(\Delta m_{\rm N} + \Delta m_{\rm F})/2$. The line indicates the 'mean' relation adopted in order to correct the individual consortia values before the merging.*

errors. Because some solutions were taken from one consortium only, it was nevertheless necessary to determine the systematic differences and apply half the difference, with opposite signs, to each solution.

A significant systematic difference was found in Δm. Figure 13.16 is a plot of $\Delta m_{\rm N} - \Delta m_{\rm F}$ versus $\Delta m \equiv (\Delta m_{\rm N} + \Delta m_{\rm F})/2$ for single-pointing doubles with relative astrometry in good agreement; subscripts N and F indicate the consortia. There is a considerable scatter, which is also strongly asymmetric, making it difficult to define a mean relation. The adopted relation, shown by the polygon line, corresponds to the ridge of the two-dimensional distribution. The systematic differences are small (≤ 0.02 mag) for $\Delta m <$ 2.5 mag, but increases rapidly for doubles with a larger intensity ratio. There is no clear trend of this effect with separation, except for very small separations ($\varrho \leq 0.3$ arcsec): in this regime the increasing correlation between the estimation errors in ϱ and Δm, combined with selection limits in both parameters, introduces statistical biases which should not be corrected.

A comparison of separations shows some systematic differences for the close binaries (Figure 13.17). Again, statistical biases related to the correlations between ϱ and Δm may play a role, and it should also be remembered that $\varrho = (X^2 + Y^2)^{1/2}$ in general has a positive bias depending on the random errors in X and Y. Moreover, since the FAST/NDAC averaging is made in the relative coordinates X, Y, the merged ϱ does not necessarily fall between $\varrho_{\rm N}$ and $\varrho_{\rm F}$. Because of the generally good agreement and the difficulty in interpreting the small differences, no systematic corrections were applied to the separations.

The position angles θ were much easier to compare than both Δm and ϱ, because the distribution of differences could be expected to be completely symmetric. Rather late in the merging a significant bias was nevertheless discovered, corresponding to a mean (or median) difference of $\theta_{\rm N} - \theta_{\rm F} = -315 \pm 15$ arcsec for the single-pointing

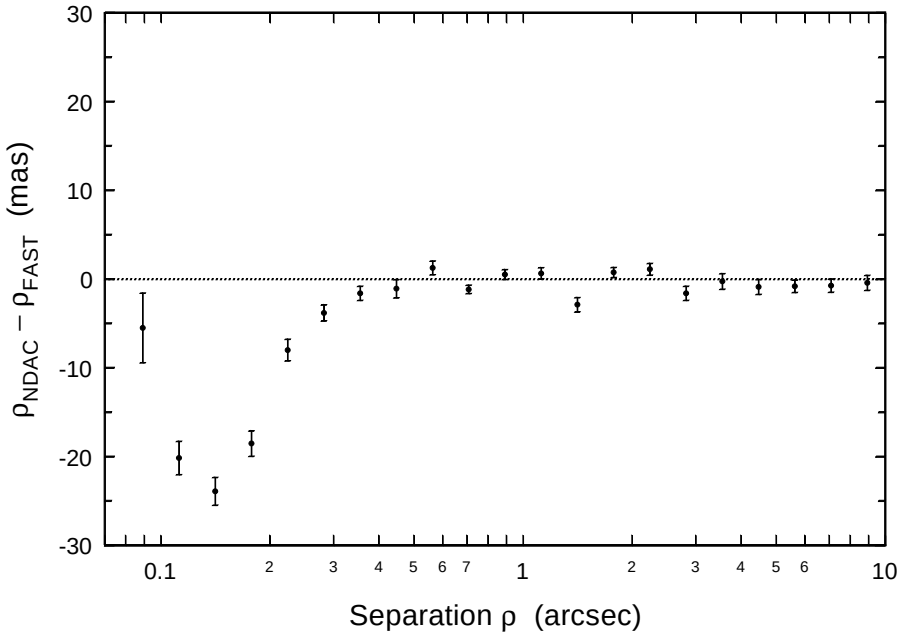

Figure 13.17. *Comparison of FAST and NDAC separations for double stars with relative astrometry in good agreement. Each point gives the mean value of $\varrho_N - \varrho_F$ for systems as a function of $\varrho = (\varrho_N + \varrho_F)/2$ in an interval of 0.1 dex. The error bars give the $\pm 1\sigma$ uncertainty of the mean value.*

systems (Figure 13.18). The source of this discrepancy was positively identified in one of the reduction chains, as being due to the neglected physical misalignment of the grid with respect to the beam combiner. Both the sign and size of the discrepancy agrees completely with the expected effect calculated from the instrument parameter g_{01} (a quantity which varied between −325 and −333 arcsec over the mission). In this exceptional case, the data were therefore unilaterally corrected by a fixed amount (330 arcsec), after which no significant systematic difference remained in the position angles.

No significant biases were found in any other parameter. In particular the differences in absolute astrometry, including the parallaxes, showed no systematic dependence on other parameters such as primary magnitude, colour, separation, or magnitude difference.

Random Differences

The statistical analysis of the random differences between the FAST and NDAC estimates of various quantities played a fundamental role in the merging process. From this analysis certain correction factors were derived for the standard errors of the consortia estimates, and these factors in turn affected the standard errors assigned to the merged (averaged) data. This correction process depends however rather critically on the assumed statistical correlation between the consortia estimates. The point is illustrated by the following example:

Suppose that a certain quantity (x) is estimated by both consortia with the same, but unknown, standard error σ. Furthermore, let ρ be the assumed statistical correlation

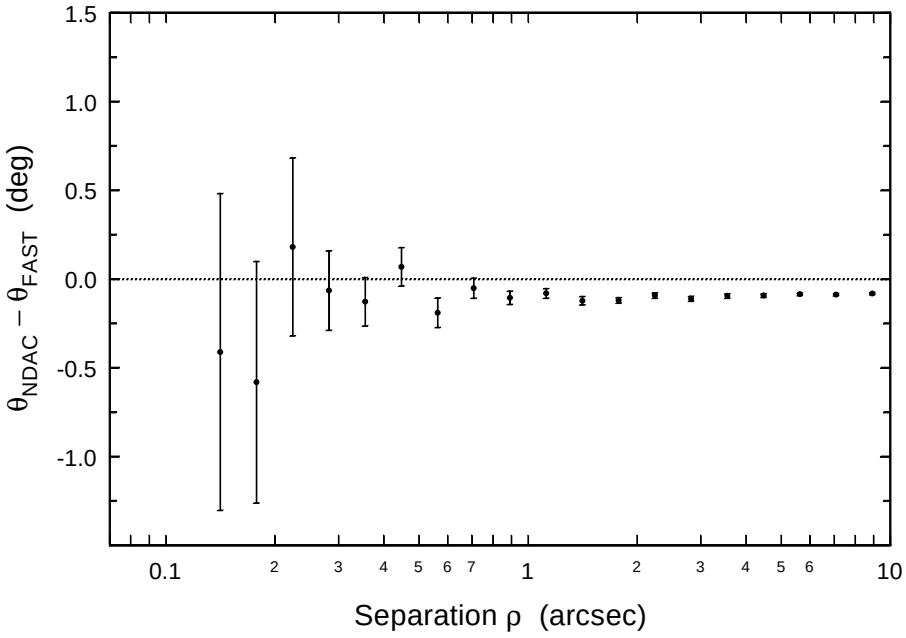

Figure 13.18. *Comparison of FAST and NDAC position angles (before correction of the bias) for double stars with relative astrometry in good agreement. Each point gives the mean value of* $\theta_N - \theta_F$ *for systems with* $\varrho = (\varrho_N + \varrho_F)/2$ *in an interval of 0.1 dex. The error bars give the* $\pm 1\sigma$ *uncertainty of the mean value.*

between the two estimates x_F and x_N. The expected variance of the difference $d = x_N - x_F$ is given by $\sigma_d^2 = 2(1-\rho)\sigma^2$. Since this variance may be estimated from a homogeneous sample of differences, the standard error of the individual estimates can be calculated as $\sigma = \sigma_d / \sqrt{2(1-\rho)}$. The merging results in the mean quantity $m = (x_N + x_F)/2$, with variance $\sigma_m^2 = \sigma^2(1+\rho)/2$. Consequently the standard error of the merged result may be calculated as $\sigma_m = (\sigma_d/2)\sqrt{(1+\rho)/(1-\rho)}$. Clearly this estimate depends strongly on the assumed ρ, especially when the latter is close to +1.

Unfortunately the correlation coefficient cannot in general be reliably estimated, except when external data of comparable (and known!) precision are available for comparison. Speckle data for the relative positions of close binaries provide a possibility, but no such analysis has been made. Only in one instance during the double-star merging was it possible to estimate a correlation between the FAST and NDAC results, without introducing too many assumptions. This concerned the relative motion of the components: $\dot{X}$, $\dot{Y}$ in FAST, and u_{11}, u_{12} in NDAC. For binaries with a small parallax, no actual relative motion is expected and the observed values could then be fully attributed to measurement noise. In this case a mean correlation coefficient of $\rho = 0.3$ to 0.4 was derived. For the astrometry of single stars, correlation coefficients around 0.7 were typically found. Lower values should be expected for the double stars in view of the much greater differences in methodology for these objects. The single-star correlations may on the other hand be approached for the absolute astrometry, e.g. of the photocentres of close binaries. Thus, reasonable values for the interconsortia correlations of the double-star parameters fall in the interval from 0.3 to 0.7.

Even assuming a rather small correlation ($\simeq$ 0.3), the observed scatter of differences in a diagram like Figure 13.16 clearly indicates that the consortia underestimated their standard errors, at least for the relative double-star parameters. Correction factors of 2 to 2.5 in $\sigma_{\Delta m}$, and of 1.5 to 1.6 in the standard errors of the relative positions, were required

in order to reconcile the FAST and NDAC solutions within their expected differences. For the absolute astrometry the situation was much better, and the standard errors in position were even somewhat overestimated by FAST.

Along these lines, the random differences in each parameter were extensively analysed, mainly as functions of magnitude and quality ratings. A set of assumed correlations and calculated correction factors resulted, which were then systematically applied to the consortia standard errors before computing the standard errors of the merged data.

Merging of the Double-Star Data

After application of systematic corrections (in Δm only) and correction factors to the standard errors, a file of the merged (averaged) relative parameters was first produced. This was used for the definitive cross-identification with the CCDM Catalogue, resulting in the system and component designations given in the Hipparcos Catalogue. It was also used to correct the photometry of the double stars for the influence of the secondary (Volume 1, Section 1.3.2). The next step of the merging was to compute the astrometric parameters and magnitudes of each component, independently from each consortium, and hence the parameters of the neutral points and the full covariance matrices. This resulted in two files, each basically containing all the data needed for the final catalogue. The final step was then the averaging of these two files for their intersection, and the copying of the remaining data to a third file. This was directly generated in the format of the machine-readable Double and Multiple Systems Annex, Part C.

13.8. Conclusions

The double star treatment of the Hipparcos data is a significant by-product of the astrometric mission. The results collected in the various sections of the Double and Multiple Stars Annex will have far-reaching consequences on the future of astronomical research in this area, both because of the homogeneous sampling of the bright double stars, including the discovery of thousands of new or suspected non-singles, and because of the important and accurate new data given for these objects, such as the parallaxes and magnitude differences. Several ground-based programmes over the coming years will help to consolidate and extend the Hipparcos conclusions on an already sifted sample.

F. Mignard, S. Söderhjelm, J. Kovalevsky, L. Lindegren